Global profiling of synaptic autoantibodies reveals a mode of action of anti-LGI1 autoantibodies in limbic encephalitis

Toshika Ohkawa

Doctor of Philosophy

Department of Physiological Sciences, School of Life Sciences
The Graduate University of Advanced Studies (SOKENDAI)

And

Division of Membrane Physiology
National Institute for Physiological Sciences, Okazaki, Japan

2014

Acknowledgements

I gratefully acknowledge my research advisers Drs. Masaki Fukata and Yuko Fukata for all their support and advice for my PhD study. I thank the members of Fukata laboratory, Norihiko Yokoi, Shinichiro Oku, Atsushi Sekiya, Tatsuro Murakami, Naoki Takahashi, Yumi Suzuki, and Mie Watanabe for kind supports.

I appreciate cooperation with many scientists, Drs. Osamu Watanabe and Hiroshi Takashima (Kagoshima University, Japan) for collecting patient serum samples and providing clinical assessment, Drs. Masahiko Watanabe, Miwako Yamasaki, and Taisuke Miyazaki (Hokkaido University, Japan) for collaborating on immunohistochemistry of LGI1$^{-/-}$ mice using specific anti-GluA1 antibodies and on double-fluorescent *in situ* hybridization of LGI1/ADAM22, Drs. Gen Sobue and Yu Miyazaki (Nagoya University, Japan) for clinical information, Dr. Elior Peles (Weizmann Institute, Israel) for CASPR2 plasmid, Kazusa DNA Research Institute and Dr. Yoshihiro Kubo [National Institute for Physiological Sciences (NIPS), Japan] for DPP10 cDNA, Dr. Bernhard Lüscher (Pennsylvania State University) for $GABA_A$ receptor γ2 plasmid, Drs. Yasuhiko Minokoshi, Kenta Kobayashi, and Shiki Okamoto (NIPS, Japan) and Drs. Roger A Nicoll and Kathryn L Lovero (University of California San Francisco) for helpful discussion, and the physicians for providing serum samples and clinical information from patients. I am very grateful to all of the patients and their families.

I would like to thank my dissertation committee members, Drs. Yumiko Yoshimura and Junichi Nabekura (NIPS, Japan) and Dr. Katsuhiko Tabuchi (Shinshu University,

Japan), for spending their time on my dissertation and for their constructive comments.

Lastly, I also thank my family for always supporting and encouraging me.

Table of Contents

Results

Summary

More than 30 mutations in LGI1, a secreted neuronal protein, have been reported with autosomal dominant lateral temporal lobe epilepsy (ADLTE). Although LGI1 haploinsufficiency is thought to cause ADLTE, the underlying molecular mechanism that results in abnormal brain excitability remains mysterious. Here, I focused on a mode of action of LGI1 autoantibodies associated with limbic encephalitis (LE), which is one of acquired epileptic disorders characterized by subacute onset of amnesia and seizures. I comprehensively screened human sera from patients with immune-mediated neurological disorders for LGI1 autoantibodies, which also uncovered novel autoantibodies against seven cell-surface antigens including DCC, DPP10, $GABA_A$ receptor, and ADAM23. My developed ELISA arrays revealed a specific role for LGI1 antibodies in LE, and concomitant involvement of multiple antibodies including LGI1 antibodies in neuromyotonia, a peripheral nerve disorder. LGI1 antibodies associated with LE specifically inhibited the ligand-receptor interaction between LGI1 and ADAM22/23 by targeting the EPTP repeat domain of LGI1, and reversibly reduced synaptic AMPA receptor clusters in rat hippocampal neurons. Furthermore, I found that disruption of LGI1-ADAM22 interaction by soluble extracellular domain of ADAM22 was sufficient to reduce synaptic AMPA receptors in rat hippocampal neurons, and that levels of AMPA receptor were greatly reduced in the hippocampal dentate gyrus in the epileptic LGI1 knockout mouse. Thus, either genetic or acquired loss of the LGI1-ADAM22 interaction reduces the AMPA receptor function to cause epileptic disorders. These results suggest that by finely regulating the synaptic AMPA receptors, LGI1-ADAM22 interaction maintains physiological brain excitability throughout life.

Furthermore, I characterized the mode of action of autoantibodies against $GABA_A$ receptor, which was the only ion channel among the autoantigens newly identified in this study. Anti-$GABA_A$ receptor autoantibodies were detected in two patients with LE and were directed against the extracellular epitope of β3 subunit of $GABA_A$ receptor. The β3 subunit-containing $GABA_A$ receptor was the primary target of patients' serum antibodies in rat hippocampal neurons, as the serum reactivity to the neuronal surface was abolished when β3 subunit was knocked-down. Application of the patient serum to rat hippocampal neuron cultures greatly decreased both synaptic and surface $GABA_A$ receptors. In conclusion, this study establishes that LGI1 autoantibodies exclusively cause LE by neutralizing LGI1-ADAM22 interaction that controls AMPA receptor function, and first reports anti-$GABA_A$ receptor encephalitis.

Introduction

Epilepsy is a worldwide and devastating brain disorder that is characterized by recurrent seizures. Most inherited forms of epilepsy result from mutations in ion channels, which directly regulate the excitability of neurons (Noebels, 2003; Steinlein, 2004). In contrast, LGI1 is a monogenic human epilepsy-related gene (Gu et al., 2002; Kalachikov et al., 2002; Morante-Redolat et al., 2002) that encodes a secreted neuronal protein (Senechal et al., 2005). Mutations in LGI1 are linked to autosomal dominant lateral temporal lobe epilepsy [ADLTE, also known as autosomal dominant partial epilepsy with auditory features (ADPEAF)], which is a rare inherited epileptic syndrome characterized by partial seizures with acoustic or visual hallucinations (Kegel et al., 2013). Many LGI1 mutations reported in ADLTE patients prevent their secretion in cultured cells, suggesting that LGI1 haploinsufficiency is a pathogenic basis for LGI1-mediated ADLTE (Senechal et al., 2005; Fukata et al., 2006; Nobile et al., 2009). Consistent with human genetic evidence, LGI1 homozygous knockout (KO) mice display repeated generalized seizures and premature death (Chabrol et al., 2010; Fukata et al., 2010; Yu et al., 2010). LGI1 heterozygous KO mice exhibit increased susceptibility to seizure-inducing stimuli (Chabrol et al., 2010; Fukata et al., 2010).

Despite definitive genetic evidence, the pathophysiological function of LGI1 in the brain remains controversial. So far, three molecular functions of LGI1 have been proposed: 1) LGI1 prevents the inactivation of the Kv1 voltage-gated potassium channels (VGKC) through the cytoplasmic regulatory protein, Kvβ (Schulte et al., 2006); 2) LGI1 regulates the neuronal development of glutamatergic circuits in the hippocampus (Zhou et al., 2009); and 3) LGI1 interacts with the epilepsy-related

ADAM22/23 transmembrane proteins and regulates AMPA receptor (AMPAR)-mediated synaptic transmission in the hippocampus (Fukata et al., 2006; Fukata et al., 2010).

The pivotal role of LGI1 in epileptic disorders was further expanded with the recent discovery of LGI1 autoantibodies in patients with autoimmune limbic encephalitis (LE), which is characterized by amnesia and seizures (Irani et al., 2010; Lai et al., 2010). LGI1 antibodies were also detected in immune-mediated peripheral nerve disorders, neuromyotonia (NMT: characterized by peripheral nerve hyperexcitability) and Morvan syndrome (MoS: characterized by peripheral nerve hyperexcitability with neuropsychiatric features) (Irani et al., 2010; Irani et al., 2012). Although autoimmune synaptic disorders including LE are thought to involve autoantibody-induced dysfunction of target ion channels, such as NMDA receptor (NMDAR) (Dalmau et al., 2008; Hughes et al., 2010) and AMPAR (Lai et al., 2009), the mode of action of LGI1 antibodies remains unknown.

Here, I aimed to clarify a pathogenic role and a mode of action of LGI1 antibodies in LE. I demonstrate that LGI1 antibodies play an exclusive role in the pathogenesis of LE and disrupt the ligand-receptor interaction of LGI1 with ADAM22 or ADAM23, resulting in reversible reduction in synaptic AMPARs. This study establishes a direct biological role of LGI1 antibodies in causing LE, and highlights importance of the LGI1-ADAM22 interaction in regulating brain excitability and probably memory storage.

Materials and Methods

The experiments using human sera were reviewed and approved by ethic committees at NIPS and Kagoshima University, and written informed consent was obtained from all patients or their family members. All animal studies were reviewed and approved by the ethic committees at NIPS and Hokkaido University and were performed according to the institutional guidelines concerning the care and handling of experimental animals.

Study population

In this study, 1,199 serum samples were collected from patients who were diagnosed with or suspected of immune-mediated disorders of the central nervous system or peripheral nervous system. These patients were seen by the authors or by clinicians at other institutions (from 72 centers in Japan) between January 4, 2006 and December 25, 2011. Diagnoses were categorized into three groups: LE, NMT/MoS, and other neurological disorders that may have autoimmune etiology (Others). To obtain serum samples with LGI1 autoantibodies (Irani et al., 2010; Lai et al., 2010), sera were tested for the presence of VGKC-complex antibodies and categorized into two groups as previously described (Kleopa et al., 2006; Irani et al., 2010): positive (titers ≥ 400 pM) or negative (titers < 400 pM). All VGKC-complex antibody-positive (69 cases including 39 LE, 19 NMT, 2 MoS, and 9 Others) samples were selected (**Table 1, 2**). In addition, 76 patients of the VGKC-complex antibody-negative group were randomly selected (20 LE, 14 NMT, and 42 Others) because the VGKC-complex antibody-negative group may still have known (such as LGI1) or unknown autoantibodies. Then, serum samples from a total of 145 patients (78 males and 67 females) with LE (59), NMT (33), MoS (2), and Others (51) were sent to NIPS via

Kagoshima University and analyzed (further detailed information on 145 patients tested in this study was summarized in **Table 1**). Patients categorized into Others positive for VGKC-complex antibodies included intractable epilepsy (2), Hashimoto's encephalopathy (2), cramp-fasciculation syndrome (1), encephalopathy (1), encephalitis (1), NMDAR encephalitis (1), and myasthenia gravis (MG) (1). Patients categorized into Others negative for VGKC-complex antibodies included encephalitis (16), encephalopathy (7), cramp-fasciculation syndrome (5), NMDAR encephalitis (3), epilepsy (3), meningitis (3), MG (1), medial temporal sclerosis (2), Hashimoto's encephalopathy (1) and stiff-person syndrome (1). For the cell-based binding assay and ELISA testing, I also used serum samples from 22 patients with neurodegenerative diseases as controls (10 males and 12 females) because they were diagnosed during the same study period, and autoimmunity has not been linked to the incidence of neurodegenerative diseases. These control diseases included amyotrophic lateral sclerosis (7), spinocerebellar degeneration (6), multiple system atrophy (5), Parkinson's disease (2), corticobasal degeneration (1), and frontotemporal lobar degeneration (1) (**Table 2**). Since 2 of 22 patients with neurodegenerative diseases were positive for DCC-ELISA, I tested 23 healthy individuals (age 24–46) as additional controls (12 males and 11 females) (**Table 2**).

Antibodies

The antibodies used in this study included: rabbit polyclonal antibodies to GluA1 (extracellular epitope; PC246, Calbiochem), GluA1 (Yamazaki et al., 2010), GluA1 (Millipore), LGI1 (ab30868, Abcam), ADAM22 (ab56118, Abcam), HA (Y-11, Santa Cruz Biotechnology), HA (561, MBL), Prox1 (ab11941, Abcam), $GABA_A$ receptor $\alpha 2$

(Rockland), α5 (Millipore), β3 (Abcam), and γ2 (extracellular epitope; Synaptic Systems); guinea pig polyclonal antibodies to vGluT1 [for Figure 6 (AB5905, Millipore) and Figure 7 (Miyazaki et al., 2003)] and vGAT (Synaptic Systems); mouse monoclonal antibodies to DCC (ab16793, Abcam), PSD-95 (MA1-046, Thermo), FLAG (M2, Sigma-Aldrich), GAD67 (1G10.2, Millipore), and $GABA_A$ receptor α1 (NeuroMab), β1 (NeuroMab), β2/β3 (extracellular epitope; Millipore), β-catenin (BD Biosciences), gephyrin (Synaptic Systems) and N-cadherin (BD Biosciences) ; and a rat monoclonal antibody to FLAG (NBP1-06712, Novus Biologicals). Rabbit polyclonal antibodies to ADAM22 were raised against GST-ADAM22-C1 (aa 757–857) for the immunoprecipitation and GST-ADAM22-C2 (aa 858–898) for the immunofluorescence analysis. A rabbit polyclonal antibody to ADAM23 was raised against GST-ADAM23 (aa 815-829). These antibodies were affinity purified on a CNBr-activated Sepharose 4B (GE Healthcare) column containing an immunizing antigen.

Plasmid construction

The cDNA of rat $GABA_A$ receptor α1 (NM_183326), α2 (NM_001135779), α5 (NM_017295), β1 (NM_012956), and β3 (NM_017065), and TMEM132A (NM_178021) was cloned from rat brain total RNA by RT-PCR. cDNAs of human DCC (pFIKE0067) and human Netrin-1 (IOH81706) were purchased from Promega and Invitrogen, respectively. Dr. Bernhard Lüscher (Pennsylvania State University) kindly provided pRK5:Myc-$GABA_A$ receptor γ2 (Fang et al., 2006). Human ODZ1 (BC140783) and human CSMD1 (BC156304) cDNAs were purchased from Thermo Fisher Scientific. Human DPP10 (KIAA1492) cDNA was provided by the Kazusa DNA Research Institute (Chiba, Japan) and Dr. Yoshihiro Kubo (NIPS, Japan). These cDNAs

were subcloned into pCAGGS vector and tagged with HA or FLAG. To construct pcDNA3.1:LGIs-FLAG-GPI, the GPI sequence (91–116 aa) of mouse Lynx1 (NM_011838) was added to the C-terminus of rat LGIs-FLAG (Fukata et al., 2006; Fukata et al., 2010). To generate the chimeric constructs LRR1-EPTP3 and LRR3-EPTP1, either LRR1 (corresponding to 1–223 aa of LGI1) and EPTP3 (221–548 aa of LGI3) or LRR3 (1–220 aa of LGI3) and EPTP1 (224–557 aa of LGI1) were fused by PCR, respectively. To generate soluble forms of ADAM22ex and ADAM23ex, the extracellular domains of mouse ADAM22ex (32–727 aa) and mouse ADAM23ex (57–787 aa) (Fukata et al., 2006) were C-terminally tagged with an HA- or Hisx6-epitope and subcloned into pAP5 vector (GenHunter). All PCR products were analyzed by DNA sequencing (Functional genomics facility, National Institute for Basic Biology, Japan). Dr. Elior Peles (Weizmann Institute) kindly provided pCi-neo:human CASPR2-HA (Poliak et al., 1999). The other LGIs and ADAMs constructs were previously described (Fukata et al., 2006; Fukata et al., 2010).

$GABA_A$ receptor β3 subunit was knocked down by the miR-RNAi system (Life Technologies). BLOCK-iT RNAi Designer was used to select the targeting sequences and the following targeting sequences were used: miR-β3-211 AGCATCGACATGGTTTCTGAA (an alternative sequence: miR-β3-347 TCTGGGTGCCTGACACATATT; both sequences yielded the same results); and miR-LacZ (β-galactosidase), GACTACACAAATCAGCGATTT as a negative control. After subcloning these oligonucleotides into pcDNA6.2-EmGFP-miR, the pre-miRNA expression cassette of pcDNA6.2-EmGFP-miR was transferred to pCAGGS vector with a chicken β-actin promoter. The resultant miR constructs were validated for the

knockdown of co-transfected $GABA_A$ receptor β3 expression in HEK293T cells by Western blotting (Fig. 11*A*).

Immunofluorescence analysis of cultured hippocampal neurons

Cultured rat hippocampal neurons (5×10^4 cells) were obtained from E18–19 embryos and seeded onto poly-L-lysine coated 12-mm cover slips in 24-well dishes. Live neurons (21–28 DIV) were incubated with the patient serum (diluted 1:100) together with the GluA1 antibody to the extracellular epitope of GluA1 for 1 h at 37°C. GluA1 staining was performed as an internal positive control. The neurons were subsequently fixed with 4% paraformaldehyde/120 mM sucrose/100 mM HEPES (pH 7.4) at room temperature for 10 min and blocked with PBS containing 10 mg/ml BSA for 15 min on ice. The bound human IgG and surface GluA1 were visualized using Cy3-conjugated and Alexa488-conjugated secondary antibodies, respectively. Fluorescent images were captured with a confocal laser scanning microscopy system (LSM5 Exciter, Carl Zeiss) equipped with a Plan Apochromat 63×/1.40 NA oil immersion objective lens. For stimulated emission depletion microscopy (STED) observation, live-labeled neurons were visualized with DyLight488-conjugated and ATTO425-conjugated secondary antibodies. The images were acquired by Leica TCS STED CW (Leica Microsystems), and the data were treated by STED deconvolution software (Leica, LAS AF).

For Figures 8*M* and 8*N*, live neurons (19 DIV) were incubated with the patient serum (#161, diluted 1:200) for 1 h at 37°C for the surface LGI1 staining. The neurons were then fixed with methanol for 10 min at -30°C and blocked with PBS containing 10 mg/ml BSA for 20 min on ice. The bound human IgG was visualized using

Alexa647-conjugated secondary antibody. The neurons were subsequently incubated with anti-GAD67 and anti-ADAM22 (or anti-ADAM23) antibodies, and stained by Cy3-conjugated and Alexa488-conjugated secondary antibodies, respectively. Fluorescent images were captured with a confocal laser scanning microscopy system (Leica TCS SP5 II) equipped with a HCX PL APO 63×/1.40 NA oil immersion objective lens combining with the Leica HyD detectors. The specificity of ADAM22 and ADAM23 antibodies was confirmed by using their KO mice (Yokoi et al., unpublished observations).

For Figure 9*D*, live neurons were incubated with the patient serum (diluted 1:200) together with anti-$GABA_A$ receptor γ2 antibody (against the extracellular epitope) for 30 min at 37°C, and labeled by Cy3-conjugated human IgG and Alexa488-conjugated rabbit IgG antibodies. Neurons were then fixed, permeabilized, and incubated with anti-gephyrin antibody, followed by staining with Alexa647-conjugated mouse IgG antibody.

Knockdown of $GABA_A$ receptor β3 subunit was performed using the miR-RNAi system as described (Fukata et al., 2013). Briefly, rat hippocampal neurons (10 DIV) were transfected with the knockdown vector by Lipofectamine 2000. At 5 days after transfection, live neurons were incubated with the patient serum (diluted 1:200) or anti-$GABA_A$ receptor β2/β3 subunit antibody (against the extracellular epitope) together with anti-γ2 subunit antibody (against the extracellular epitope) for 30 min at 37°C. The neurons were fixed and blocked with PBS containing 10 mg/ml BSA for 30 min on ice. The bound human IgG (or β3) and γ2 were visualized using Cy3-conjugated

and Alexa647-conjugated secondary antibodies, respectively. Neurons transfected with the knockdown vector were reported by co-cistronic expression of EmGFP.

Immunoprecipitation and mass spectrometry

Cultured rat hippocampal neurons (5×10^5 cells/well) were seeded in 6 well plates (3 wells/immunoprecipitation). The neurons were incubated with the patient serum (diluted 1:50) for 1 h at 37°C. The neurons were subsequently washed twice with PBS, and then lysed with buffer A (20 mM Tris-HCl [pH 8.0], 1 mM EDTA, 100 mM NaCl, 1.3% Triton X-100 and 50 μg/ml PMSF). The lysates were cleared by centrifugation at 10,000 *g* for 5 min at 4°C. The immune complexes were precipitated with Protein A Sepharose (GE Healthcare). The immunoprecipitates were separated by SDS-PAGE, and the gels were subsequently analyzed by silver staining and Western blotting. All the specific protein bands were excised from a silver-stained gel and analyzed with mass spectrometry (LC-MS/MS) as described (Fukata et al., 2010) (**Table 2, 3**). The gel pieces with the corresponding molecular weights in the control serum sample were also analyzed to rule out non-specific binding of human serum antibodies.

Cell-based binding assay

COS7 cells were seeded onto three poly-*d*-lysine coated 12-mm cover slips in each well of a 6-well plate (3×10^5 cells/well) and transfected with the indicated target candidates, including LGI1, CASPR2, ADAM23, DCC, DPP10, TMEM132A, ODZ1, CSMD1 and $GABA_A$ receptor subunits (**Table 4**; **Fig. 2**; **and Fig. 10**). To display LGI1 on the cell-surface, a GPI anchor signal was added to the C-terminus of LGI1. At 24 h after transfection, the cells were fixed with 2% paraformaldehyde at room temperature for 20

min and blocked with PBS containing 10 mg/ml BSA for 10 min on ice. The fixed cells were incubated with the patient serum (diluted 1:10) and either anti-FLAG antibody for LGI1, anti-HA antibody for DPP10 and DPP6, anti-DCC antibody, or anti-$GABA_A$ receptor γ2 at room temperature for 1 h. This incubation was followed by incubation with the Cy3-conjugated secondary antibody for human serum antibodies and the Alexa488-conjugated secondary antibody for the individual target staining. For CASPR2, ADAM23, and TMEM132A with the internal HA tag or $GABA_A$ receptor α1, α2, α5, β1, and β3 subunits, after staining surface-bound human IgG, the cells were permeabilized with 0.1% Triton X-100 for 10 min, blocked with PBS containing 10 mg/ml BSA, and incubated with the anti-HA polyclonal antibody or antibodies to individual $GABA_A$ receptor subunits, followed by staining with the Alexa488-conjugated secondary antibody. I confirmed that sera from patients did not bind to untransfected cells that did not express the candidate protein through distinguishing untransfected cells with Hoechst dye (33342, Invitrogen) nucleic acid staining, and that the patient sera as well as control sera did not bind to COS7 cells that had not been treated with Lipofectamine transfection reagent (data not shown). In addition, I confirmed that control sera from patients of neurodegenerative diseases did not bind to the candidate-antigen expressing cells (except for DCC-expressing cells).

Cell-based ELISA

HEK293T cells were plated onto 96-well plates (3×10^4 cells/well; Nunclon TC, Nunc) coated with polyethylenimine. Plasmids (0.1 μg/well for LGI1 and CASPR2, 0.06 μg/well for DCC and 0.08 μg/well for DPP10) were transfected into HEK293T cells using Lipofectamine and Plus reagent (Invitrogen). After a 24-h incubation, the cells

were treated with the serially diluted sera from patients (as shown in Fig. 3*A*) and control subjects together in the same 96-well plate for 15 min at 37°C. The cells were washed with PBS and fixed in 4% paraformaldehyde for 15 min. The cells were then washed once with PBS, twice with PBST (PBS containing 0.05% Tween 20), and blocked using Protein-Free T20 blocking buffer (Thermo) at room temperature for 1 h. Subsequently, the cells were incubated with an HRP-conjugated anti-human IgG antibody in a 1:2000 dilution for 15 min at 37°C and washed twice with PBST and once with PBS. The cell-bound human IgG was detected using Ultra-TMB substrate solution (Thermo). The colorimetric reaction was stopped upon the addition of 2 M sulfuric acid and the resulting plates were measured at 450 nm absorption with MULTISKAN FC microplate reader (Thermo). Wells containing non-transfected cells were used to subtract the background signals. I assessed the quality of the ELISA by calculating the Z-prime factors (Zhang et al., 1999). The Z-prime factors of the LGI1, CASPR2, DCC and DPP10 ELISAs were 0.88, 0.77, 0.61 and 0.67, respectively; therefore the individual ELISA tests were considered to be excellent assays (Z-prime factor > 0.5). The cut-off value, which discriminates the positive results from the negative results, was determined by collating with my cell-based binding assay results. Samples were regarded as positive if their values of ELISA were over 0.5, 0.3, 0.3, and 0.4 for LGI1, CASPR2, DCC and DPP10, respectively. Laboratory investigators performed all the procedures of ELISA test without knowing clinical features and diagnoses of samples. I used the absolute ELISA values of serum samples as predictor variables, and clinical features and diagnoses of patients as outcomes. I categorized clinical features and diagnoses of patients into eight and three groups, respectively, and examined the association of ELISA results (positive or negative) with them (**Table 5**). The ELISA

test for LGI1 should be useful for the clinical diagnosis of autoimmune-mediated LE with a high specificity (94.2%), sensitivity (49.2%) and positive predictive value (85.3%) at the 0.8 cut-off point. In addition, the chi-square test showed a significant difference in the frequencies of LE between patients with the LGI1 antibody (cut-off value, 0.8) and all 145 patients (P = 1.19E-07) (**Table 6**).

Tests of effects of LGI1 autoantibodies

To prepare the recombinant soluble form of ADAM22ex-HA or ADAM23ex-HA, at 24 h after transfection HEK293T cells were further cultured in serum-free DMEM for three days to mediate the secretion of recombinant proteins into the medium. Subsequently, the conditioned medium was collected and used as soluble ADAM22ex or ADAM23ex. COS7 cells were transfected with LGI1-FLAG-GPI to display LGI1-FLAG on the cell-surface. At 24 h after transfection, the cells were incubated with either control serum or patient serum containing LGI1 antibodies for 10 min at 37°C (1:1 diluted in DMEM). After washing, soluble ADAM22ex-HA or ADAM23ex-HA (3 nM) was applied, and the cells were incubated for 1 h at 4°C. The cells were washed and fixed with 2% paraformaldehyde. The bound ADAMex-HA and surface-expressed LGI1-FLAG-GPI were visualized with anti-HA and anti-FLAG antibodies, followed by staining with Alexa488- and Alexa647-conjugated secondary antibodies, respectively. In addition, the bound serum antibodies were visualized by the Cy3-conjugated secondary antibody. Fluorescent images were taken with a confocal laser microscopy system. A similar experiment was performed using secreted Netrin-1-FLAG and DCC for Figures 4*C* and 4*D*. To quantify the intensity of surface ADAM22ex-HA and LGI1-FLAG expression, I randomly chose 15 cells from three independent experiments

and measured the mean intensities. The ratio of the ADAM22ex-HA intensity to LGI1-FLAG-GPI intensity was graphed.

To examine the effect of LGI1 antibodies in neurons, rat cultured hippocampal neurons (12 DIV) were treated with disease control serum (Control #19) or the serum from an LE patient (#161) for three days. Ten μl of fresh serum was added daily to 500 μl of each culture medium (final 6% concentration). Subsequently, endogenous ADAM22 was immunoprecipitated by ADAM22 antibody (targeting ADAM22 cytoplasmic tail)-conjugated beads. M-280 Tosylactivated Dynabeads (Invitrogen) were used for antibody-conjugation according to manufacturer's instructions. The isolated immune complex was separated by SDS-PAGE and analyzed by Western blotting with anti-ADAM22 and anti-LGI1 antibodies. For the quantification, ImageJ software (NIH) was used.

To examine the effect of LGI1 antibodies (or soluble form of ADAM22, ADAM22ex-HA) on synaptic AMPARs, cultured hippocampal neurons (12 DIV) were treated with disease control serum (Control #19), the serum from an LE patient (#161) or ADAM22ex-HA (~200 nM) for 3 days, as described above. To examine the reversibility of the inhibitory effect of LGI1 antibodies on synaptic AMPARs, the serum-containing medium was replaced with serum-free medium after the three-day incubation and neurons were further incubated for 24 h. Subsequently, live neurons were incubated with a GluA1 antibody for 15 min at 37°C. After fixation, the surface-expressed GluA1 was visualized with the Cy3-conjugated antibody. The neurons were then permeabilized with 0.1% Triton X-100 for 10 min, blocked with PBS

containing 10 mg/ml BSA and incubated with anti-PSD-95 and anti-vGluT1 antibodies, followed by staining with Alexa488-conjugated and Alexa647-conjugated secondary antibodies, respectively. To quantify the synaptic expression of AMPARs, I randomly chose 36 dendrites (20 μm length) from 3 independent neuronal cultures and analyzed the number and intensity of GluA1 clusters. Synaptic GluA1 puncta, which were adjacent to both vGluT1 and PSD-95 and bigger than 1/π μm in diameter (threshold was set at 70 arbitrary units of mean fluorescent intensity), were counted. The quantification of PSD-95 puncta apposed to vGluT1 was analyzed by the same criteria. Microscope control and all image analysis were performed with Carl Zeiss ZEN software.

Immunohistochemistry

For Figure 6*A*, brains of LGI1 KO ($LGI1^{-/-}$) (P18) mice (Fukata et al., 2010) and their littermate controls were freshly obtained after euthanasia and immediately frozen. Sections (10 mm) immunoreacted with the patient serum (#161, diluted 1:500) and anti-Prox1 were incubated with Cy3- and Alexa488- conjugated secondary antibodies. Detailed procedures were described previously (Fukata et al., 2013). Images were taken as described for immunofluorescence of neurons.

For Figure 7, $LGI1^{-/-}$ (P20) mice and their littermate controls were anesthetized by pentobarbital (75 mg/kg, i.p.) and perfused with 4% paraformaldehyde in 0.1 M PB. Pairs of mutant and control brains were embedded in single paraffin blocks. Paraffin sections (4 μm in thickness) were successively incubated with 1 mg/ml pepsin in 0.2 N HCl at 37°C for 6 min (Watanabe et al., 1998), 10% normal donkey serum for 20 min, primary antibodies diluted in PBS (anti-GluA1, 1μg/ml; vGluT1, 1μg/ml) overnight,

biotinylated secondary antibodies (1:200, Jackson Immunoresearch) for 2 h, and streptavidin-peroxidase (Nichirei Corp.) for 30 min. Immunoreaction was visualized using the tyramide signal amplification kit with fluorescein tyramide (PerkinElmer Life Sciences). Images were taken using an epifluorescence stereomicroscope equipped with a digital camera (DP70; Olympus).

In situ *hybridization*

Complementary DNA fragments of mouse vGluT1 (nucleotides, 301–1680; GenBank accession number, BC054462), mouse GAD67 (1036–2015; NM_008077), mouse LGI1 (1–503; NM_020278), mouse ADAM22 (1351–1960; HM004095), and mouse ADAM23 (1991–2490; NM_011780) were subcloned into the pBluescript II and used for the preparation of fluorescein-labeled cRNA probes. Adult C57BL/6 mice were used. Subsequent detailed procedures were described previously (Yamasaki et al., 2010).

Tests of effects of $GABA_A$ receptor autoantibodies

To examine the effect of $GABA_A$ receptor antibodies on the surface or synaptic $GABA_A$ receptors, cultured rat hippocampal neurons (~30 DIV) were treated with control serum or the patient serum containing $GABA_A$ receptor autoantibodies for 2 or 3 days. Six μl of the serum was added daily to 300 μl of each culture medium (final 4 or 6% concentration). Live neurons were incubated with an antibody to an extracellular epitope of $GABA_A$ receptor γ2 for 15 min at 37°C. After fixation, the surface-expressed γ2 subunit was visualized with the Cy3-conjugated antibody. After permeabilizing and blocking neurons, the neurons were incubated with anti-gephyrin and vGAT antibodies, followed by staining with Alexa488- and Alexa647-conjugated secondary antibodies,

respectively. Serum-treated sister cultures were also independently stained with anti-$GABA_A$ receptor β3 subunit antibody (the intracellular epitope, Abcam) after cell-permeabilization to visualize the $GABA_A$ receptors containing β3 subunit. To quantify the synaptic $GABA_A$ receptors, we randomly chose 12 dendrites (20 μm length) from 3 independent neuronal cultures and analyzed the number of $GABA_A$ receptor γ2 and β3 clusters. Synaptic γ2 and β3 puncta, which were adjacent to both vGAT and gephyrin and bigger than $1/\pi$ μm in diameter (threshold was set at 70 arbitrary units of mean fluorescent intensity), were counted. The quantification of gephyrin puncta apposed to vGAT was analyzed by the same criteria. Microscope control and all image analysis were performed with Carl Zeiss ZEN software.

Biotinylation of cell-surface proteins was performed as previously (Hughes et al., 2010). Briefly, neurons were incubated with 2.3 mM Sulfo-NHS-Biotin (Thermo) for 30 min at 4°C. Neurons were then incubated with quenching buffer containing 100 mM glycine for 30 min and lysed in buffer A containing [20 mM Tris-HCl (pH 8.0), 1 mM EDTA, 100 mM NaCl, 1% SDS and 50 μg/ml PMSF]. After 20 min extraction, the lysates was diluted with 10 vol of buffer A containing 1% Triton-X-100 instead of SDS. After centrifugation at 20,000 *g* for 20 min, the supernatant was incubated with NeutrAvidin agarose beads (Thermo) for 12 hr at 4°C. The isolated surface proteins were separated by SDS-PAGE and analyzed by Western blotting with indicated antibodies. For the quantification, ImageJ software (NIH) was used.

Statistical analysis

Statistical comparisons between two groups or multiple groups were performed by the

Student's *t*-test or one-way ANOVA with Tukey's or Dunnett's post hoc analysis, respectively. Fisher's two-sided exact test was used for Table 5. Box-and-whisker plots are shown to identify the median, 25th, and 75th percentiles as well as the extremes.

Results

1. The mode of action of anti-LGI1 autoantibodies

1-1. Screening patient sera with immune-mediated neurological disorders for LGI1 autoantibodies

To select the sera containing LGI1 autoantibodies and cover as many autoantibodies involved in LE or NMT as possible, I analyzed serum samples from 145 patients who were diagnosed with immune-mediated neurological disorders including LE, NMT, MoS, and Others (**Table 1**; see Materials and Methods). I screened serum antibodies for binding to the cell surface of cultured rat hippocampal neurons (the identity between human and rat LGI1 proteins is 97%). The serum from 48 patients bound to the neuronal cell surface (**Table 2**) and showed various staining patterns (**Fig. 1*A***), suggesting that these target antigens were different. Target proteins were then immunoprecipitated from cultured neurons with the bound serum antibodies and identified using mass spectrometry (**Fig. 1*B* and Table 2, 3**; see also Fig. 9*A*). Specific proteins were immunoprecipitated by individual sera: for example, the serum #149, #1, and #53 immunoprecipitated protein bands of 60, 170, and 100 kDa; and they were identified as LGI1, CASPR2, and GluA subunits of AMPARs, respectively. In addition to these previously reported antigens, I identified several novel candidates including DPP10 (dipeptidyl-peptidase 10; 90 kDa), DCC (Deleted in colorectal carcinoma; 180 kDa), CSMD1 (Cub and sushi multiple domains 1; > 300 kDa), ODZ1/4 (odd Oz/ten-m homolog 1/4; > 300 kDa), TMEM132A (transmembrane protein 132A; 160 kDa) (**Fig. 1*B***), and $GABA_A$ receptor α1 (48 kDa) (**Fig. 9*A***). I noted that some serum antibodies isolated more than one protein. For example, CASPR2, DPP6, and DPP10 were detected in the immunoprecipitate of serum #27 (**Fig. 1*B***). However, it is not

sufficient to conclude that these patients have multiple antibodies against different proteins, because some proteins might be coimmunoprecipitated with the target antigen.

Using the cell-based binding assay with heterologous cells, I next determined the direct cell-surface antigens of serum antibodies. The identified candidate proteins were displayed on the surface of COS7 cells and the cells were incubated with the patient's serum. To display a secretory protein LGI1 on the cell-surface, a glycosylphosphatidylinositol (GPI) anchor signal was added to the C-terminus of LGI1. I confirmed the presence of known autoantibodies against LGI1, GluA2 and CASPR2, and determined several novel autoantibodies against: 1) DCC, a receptor for axon guidance molecule Netrin-1 (Horn et al., 2013); 2) DPP10, an auxiliary subunit of Kv4.2 (Lai and Jan, 2006); 3) ADAM23, one of receptors for LGI1 (Fukata et al., 2006); 4) CSMD1, a neuronal transmembrane protein associated with schizophrenia (Ripke et al., 2011); 5) ODZ1, a neuronal transmembrane protein; 6) TMEM132A, an uncharacterized transmembrane protein (Oh-hashi et al., 2010); and 7) $GABA_AR$ subunits (**Fig. 2*A, D*** and **Table 4**; see also Fig.9*A*, *B*). Some patients had antibodies against more than one target antigen (**Fig. 2*B***). Although DPP6 and DPP10 co-existed at similar levels in the immunoprecipitates from neurons (**Fig. 1*B***), and both of them interact with the transmembrane segment of Kv4.2, a voltage-gated potassium channel, and regulate Kv4.2 channel properties as auxiliary subunits (Lai and Jan, 2006), cell-based binding assays showed that the serum antibodies specifically bound to DPP10, but did not bind to either DPP6 or Kv4.2 (#72, **Fig. 2*C***), indicating that DPP10 is a novel autoantigen, and suggesting that DPP6 is stoichiometrically associated with DPP10 in neurons.

1-2. Cell-based ELISA arrays reveal an exclusive role for LGI1 autoantibodies in LE

To investigate the relative contribution of individual antibodies to diseases, I developed the quantitative cell-based ELISA test against LGI1, CASPR2, DCC, and DPP10, the top four of frequent autoantigens in the present screening (data not shown). The assay was specific and showed a linear correlation for dilution linearity [**Fig. 3*A***, an example of serum #4 (r = 0.936, against LGI1)]. All the serum data from 145 patients were sorted in descending order of the anti-LGI1 (**Fig. 3*B***) or anti-CASPR2 (**Fig. 3*C***) ELISA values to generate heat maps. I observed that 85.3% (29/34) of patients with high levels of LGI1 antibodies (absorbance > 0.8) had been diagnosed with LE (**Fig. 3*B*** and **Table 5**; $P < 0.0001$), and most of these LE patients (26/29, 89.7%) had only the LGI1 autoantibody (without CASPR2, DCC nor DPP10 antibodies). In contrast, 75.0% (9/12) of patients with CASPR2 antibodies (absorbance > 0.3) had been diagnosed with NMT/MoS ($P < 0.0001$) (**Fig. 3*C*** and **Table 5**), and all these patients concurrently had multiple antibodies to LGI1, DCC, and/or DPP10 (also see Fig. 2*B*). To further examine the relationship between LGI1 and CASPR2 antibodies in patients with LE or NMT, I generated a scatterplot (**Fig. 3*D***). Distinct tendencies were noted: 1) high levels of anti-LGI1 (> 0.8) were associated with LE independently of anti-CASPR2; and 2) anti-CASPR2 reactivity (> 0.3) was associated with NMT and was concurrently accompanied by moderate levels of anti-LGI1 reactivity (0.5–1.0). Importantly, retrospective investigations revealed that two of the three LE cases with CASPR2 antibodies (> 0.3) (#9 and #27, asterisks in Figure 3*C*, *D*) had experienced peripheral nerve symptoms as NMT, supporting that CASPR2 antibodies are specifically

associated with the NMT feature ($P < 0.0001$) (**Table 5**). These results indicate that among identified autoantibodies, LGI1 autoantibodies play an exclusive role in LE and strongly suggest that my established ELISA arrays can be immediately applicable to clinical practice.

On the other hand, DCC antibodies occurred in seven patients with NMT/MoS and four patients with LE, and in all these cases DCC antibodies co-occurred with CASPR2 and/or LGI1 antibodies (**Fig. 3*B***, ***C***). DCC antibodies appeared to be significantly associated with NMT/MoS (**Table 5**; $P < 0.01$). Uniquely, DCC antibodies were solely detected in one isolated MG (#144; **Table 2, 5**). DCC antibodies were also detected in other category of diseases such as multiple system atrophy and amyotrophic lateral sclerosis, but were not detected in 23 healthy controls (**Table 2**).

1-3. LGI1 autoantibodies block the binding of LGI1 to ADAM22

I next explored a mode of action of LGI1 antibodies. Of the three proposed functions of LGI1 (*see Introduction*), I first asked whether the LGI1 autoantibody directly affects the interaction of LGI1 with its major receptor, ADAM22, because there has been no evidence concerning a direct interaction between the Kv1 channel and LGI1. In addition, it seems unlikely that the autoantibody subacutely affects the development and remodeling of the neural circuits in the adult brain. When COS7 cells transfected with LGI1 tagged with FLAG-GPI were incubated with the soluble extracellular domain of ADAM22 (ADAM22ex-HA), ADAM22ex-HA specifically bound to LGI1-FLAG-GPI on the cell surface (**Fig. 4*A***). In contrast, when cells were pre-treated with the serum #8 from a patient with LE, which contains monospecific antibodies to LGI1 (absorbance

1.33 in ELISA), the interaction of LGI1 with ADAM22 was significantly inhibited in a dose-dependent manner (**Fig. 4*A***). The serum also inhibited the interaction of LGI1 with another receptor ADAM23 (**Fig. 4*A***). In addition, most of sera from patients with LE, containing monospecific LGI1 antibodies (absorbance > 0.8 in ELISA), significantly inhibited the LGI1-ADAM22 interaction (**Fig. 4*B***). Under experimental conditions, control sera and the patient serum containing CASPR2 antibodies without LGI1 antibodies (#17) did not affect the binding of LGI1 to ADAM22 (one representative control is shown from four independent control samples tested). The inhibitory effect of LGI1 antibodies was specific to the LGI1-ADAM22 interaction as the patient serum (#149) did not affect the ligand-receptor interaction of Netrin-1 with DCC (**Fig. 4*C***). In contrast, serum #144, which contained monospecific antibodies to DCC (1.59 in ELISA; a patient with MG), specifically inhibited the interaction of Netrin-1 with DCC (**Fig. 4*C***). Furthermore, some of other DCC antibodies detected in patients with NMT (#6 and #21) inhibited the Netrin-1-DCC interaction (**Fig. 4*D***).

I also examined the disease specificity of the effect of LGI1 antibodies on the LGI1-ADAM22 interaction. As shown in Figure 4*B*, the inhibitory effect of sera with monospecific LGI1 antibodies (absorbance > 0.8 in ELISA) was shared among patients with LE, but importantly not with NMT patients (#5 and #52). I reassessed the inhibitory effect of all the anti-LGI1 sera from patients with LE and NMT (absorbance > 0.5 in ELISA) (**Fig. 4*E***). Importantly, anti-LGI1 sera from patients with LE significantly inhibited the LGI1-ADAM22 binding ($P < 0.0001$), whereas anti-LGI1 sera from patients with NMT did not inhibit (not significantly different from control serum group without LGI1 antibodies). Taken together, these results strongly suggest

that the antibody-mediated inhibition of the LGI1-ADAM22 interaction is a pathogenic mechanism for LE.

I next mapped the epitope of LGI1 autoantibodies to further determine the specificity of the inhibitory effect of the serum. LGI1 has leucine-rich repeat (LRR) and EPTP repeat domains, and the EPTP repeat domain mediates ADAM22 binding (Fukata et al., 2006). LGI3, a member of LGI1 family proteins, also contains LRR and EPTP repeat domains, but does not bind to ADAM22 (Fukata et al., 2010). I generated two chimeric constructs between LGI1 and LGI3: LRR3-EPTP1, consisting of the LRR domain of LGI3 and EPTP of LGI1; and LRR1-EPTP3, derived from the LRR domain of LGI1 and EPTP of LGI3 (**Fig. 5*A***). As expected, the cell-surface binding assay showed that LGI1 and LRR3-EPTP1, but neither LGI3 nor LRR1-EPTP3, bound to ADAM22 (**Fig. 5*B***). I next asked whether serum LGI1 antibodies bind to the EPTP repeat and prevent LGI1 from interacting with ADAM22. When transfected COS7 cells were incubated with the serum from an LE patient containing LGI1 antibodies, the antibodies bound to LGI1, LRR3-EPTP1 and LRR1-EPTP3 but not to LGI3 (**Fig. 5*C***), indicating that serum contains polyclonal LGI1 antibodies and that their epitopes are distributed to both LRR and EPTP repeat domains of LGI1. Indeed, all the tested sera from patients with LGI1 antibodies showed binding to both LRR and EPTP repeat domains of LGI1 (data not shown). I found that the serum antibodies inhibited the binding of LRR3-EPTP1 to ADAM22 (**Fig. 5*D***), indicating that LGI1 antibodies neutralize the receptor binding activity of LGI1 by acting on the EPTP repeat domain of LGI1.

1-4. Loss of LGI1-ADAM22 interaction reversibly reduces synaptic AMPARs

I next investigated whether LGI1 antibodies inhibit the interaction of endogenous LGI1 with ADAM22 in hippocampal neurons. I used the serum #161, because this serum was monospecific against LGI1 (tested in **Fig. 3**: LGI1 ELISA value, 1.86; CASPR2, 0.16; DCC, 0.10; DPP10, -0.17) and showed the strongest inhibitory effect in COS7 cells (**Fig. 4*B***). Consistently, comparative immunohistochemistry with brain sections of the wild-type and LGI1 KO mice showed the selective lack of reactivity of the serum #161 in the brain of the LGI1 KO mice (**Fig. 6*A***). When ADAM22 was immunoprecipitated from cultured hippocampal neurons treated with control serum, LGI1 was efficiently coimmunoprecipitated (**Fig. 6*B***). In contrast, when neurons were pretreated with the patient serum, the amount of coimmunoprecipitated LGI1 was significantly reduced (23.7 ± 1.92% of control; $P = 0.027$; $n = 3$).

In LGI1 KO mice, AMPAR-mediated synaptic transmission is reduced in the hippocampus and lethal epilepsy inevitably occurs (Fukata et al., 2010). However, it remains unclear whether acute disruption of the LGI1-ADAM22 interaction affects synaptic AMPARs. When hippocampal neurons were treated with the patient serum for 3 days, the number of synaptic GluA1 clusters was significantly reduced ($P < 0.0001$), whereas that of PSD-95, a postsynaptic scaffolding protein, did not change (**Fig. 6*C***, ***D***). Importantly, the effect on synaptic AMPARs was reversed by removal of serum antibodies from the neuronal cultures (**Fig. 6*E***), providing a possible explanation for the improvement of LE symptoms after plasma exchange (Vincent et al., 2006; Lancaster and Dalmau, 2012). Furthermore, application of soluble ADAM22 fragment (ADAM22ex) to the neuron culture inhibited the interaction of LGI1 with endogenous ADAM22 (30.0 ± 7.3% of control; $P = 0.0036$; $n = 3$) (**Fig. 6*F***) and reduced synaptic

AMPARs ($P < 0.0001$) (**Fig. 6*G, H***), indicating that the impaired interaction of LGI1 with ADAM22 is sufficient to cause the reduction of synaptic AMPARs. Thus, the effect of the patient serum on AMPARs is specifically attributed to the LGI1 antibody-mediated inhibition of LGI1-ADAM22 interaction.

Next, I examined whether genetic deletion of LGI1, which causes lethal epilepsy in mice, affects AMPAR expression in the brain. I performed immunofluorescence examination of the LGI1 KO mouse brain using GluA1 subunit-specific antibody (Yamazaki et al., 2010). To reliably evaluate genotypic differences, a pair of littermate control ($LGI1^{+/+}$) and KO ($LGI1^{-/-}$) mouse brains at P20 were embedded in single paraffin blocks, mounted on the same glass slides, and subjected to immunohistochemical incubation under the same conditions. Overall GluA1 distribution was consistent with previously reported one (Yamasaki et al., 2011) (**Fig. 7*A***). In the hippocampal formation of control mouse brain, the neuropil of dentate gyrus, CA1 and CA3 was strongly immunostained. In the LGI1 KO mice, GluA1 immunoreactivity was robustly reduced in the dentate gyrus, particularly in the molecular layer (**Fig. 7*B***), where the immunoreactivity of ADAM22 and ADAM23 is greatly reduced (Fukata et al., 2010). Under the condition, no such changes were observed for vGluT1, a marker protein for glutamatergic axon terminals (**Fig. 7*C***).

1-5. ADAM22 and ADAM23 are expressed in inhibitory and excitatory neurons in the hippocampus

Why does the AMPAR-function reduced by the LGI1 antibodies or genetic loss of LGI1 cause seizures that result from neuronal hyperexcitation? In the hippocampus

many inhibitory interneurons constitute strong feedback or feedforward inhibition loops (Acsády et al., 1998), and the reduced activity of inhibitory interneurons may cause overall network hyperexcitability. To explore a possibility that LGI1 acts on the inhibitory neurons to regulate their AMPAR function, I first examined the cellular expression of ADAM22, ADAM23, and LGI1 mRNAs by double fluorescent *in situ* hybridization with vGluT1 or GAD67, markers of glutamatergic excitatory neurons or GABAergic inhibitory interneurons, respectively (**Fig. 8*A*–*L***). Overall, ADAM22, ADAM23, and LGI1 mRNAs were coexpressed with vGluT1 mRNA in principal excitatory neurons in CA1, CA3 and dentate gyrus of the hippocampus, except that ADAM23 mRNA was little expressed in dentate granule cells (**Fig. 8*B*, *D***, ***G***, and ***J***). At a high magnification of the dentate hilus (**Fig. 8*E*, *F***; **8*H*, *I***; and **8*K*, *L***), mRNAs of ADAM22, ADAM23, and LGI1 were coexpressed in the neurons expressing GAD67 mRNA (indicated by arrowheads), in addition to the neurons expressing vGluT1 mRNA (representing excitatory hilar mossy cells, indicated by arrows). These results indicate that inhibitory interneurons as well as excitatory neurons in the hippocampus express ADAM22, ADAM23, and LGI1.

I next examined whether LGI1 associates with ADAM22/23 on inhibitory interneurons by immunofluorescence analysis (**Fig. 8*M***, ***N***). Rat cultured hippocampal neurons were stained triply by anti-GAD67, anti-ADAM22 or anti-ADAM23, and the patient serum (#161), which was monospecific to LGI1 (**Fig. 3** and **Fig. 6*A***) and was used for the staining of surface-bound LGI1. Consistent with mRNA expression patterns, ADAM22 and ADAM23 proteins were expressed in GAD67-expressing interneurons. I found that cell-surface LGI1 signals were present as small clusters on all the neurons in the culture,

consistent with a previous report (Lai et al., 2010). The LGI1 signals were detected at the surface of both GAD67-negative and -positive neurons and colocalized with ADAM22 and ADAM23 signals at the dendrite and soma of the GAD67-positive inhibitory interneurons. These results support a hypothesis that the reduced AMPAR function in inhibitory interneurons by the reduced LGI1 function could cause disinhibition of neural networks leading to the seizure. Consistently, the autoantibodies to AMPARs produced in LE patients with seizures reduce synaptic AMPARs in cultured hippocampal neurons (Lai et al., 2009).

2. Identification and characterization of $GABA_A$ receptor autoantibodies

2-1. Identification of $GABA_A$ receptor autoantibodies in patients with LE

As described in the section 1-1, by exploring unknown synaptic autoantigens involved in LE using a non-biased proteomic method, I identified a new autoantibody against the $GABA_A$ receptor. A protein with a molecular mass of 48 kDa (p48) was specifically detected in the immunoprecipitate by serum antibodies from one patient with LE (#32), but not by control serum antibodies (**Fig. 9*A***). The molecular identity of p48 was determined by LC-MS/MS (**Fig. 9*B***). Molecular weights of seven peptide fragments derived from p48 coincided with those from rat $GABA_A$ receptor α1 subunit: LLDGYDNR, ITEDGTLLYTMR, AEVVYEWTR, SVVVAEDGSR, NNTYAPTATSYTPNLAR, GDPGLATIAK and EVKPETKPPEPK. The estimated molecular weight of rat $GABA_A$ receptor α1 (51.7 kDa) was close to that of p48. Also, peptide fragments coincided with those from $GABA_A$ receptor β3 subunit (NVVFATGAYPR and IKIPDLTDVNAIDR) were present in the same immunoprecipitate [the corresponding band (54.2 kDa) was masked by the human IgG heavy chain]. Western blotting with antibodies specific to α1, β3, and γ2 subunits of $GABA_A$ receptor confirmed the immunoprecipitation of heteropentameric $GABA_A$ receptors (**Fig. 9*C***). Consistently, the serum antibodies showed overlapped signals with inhibitory synapses marked by $GABA_A$ receptor γ2 and gephyrin antibodies in rat hippocampal neurons (**Fig. 9*D***).

2-2. $GABA_A$ receptor autoantibodies are directed to extracellular epitope of β3 subunit

To examine whether the patient serum antibodies directly bind to the $GABA_A$ receptor,

and if so, which of $GABA_A$ receptor subunits the antibodies recognize, the cell-based binding assay was performed. Because the native $GABA_A$ receptor is a heteropentamer composed of two α, two β and one γ subunits and the patient serum immunoprecipitated α1, β3, and γ2 subunits from hippocampal neurons (**Fig. 9*C***), α1, β3, and γ2 subunits were co-expressed to display heteropentameric $GABA_A$ receptors at the cell surface of COS7 cells. Then, transfected cells were fixed and incubated with the patient serum without cell permeabilization. I found that the serum antibodies from the patient (#32) robustly reacted to the surface-expressed $GABA_A$ receptors (α1/β3/γ2) (**Fig. 10*A***, the leftmost panel). Among 19 individual $GABA_A$ receptor subunits, I then focused on α1, α2, α5, β1, β3, and γ2 subunits, which constitute major hippocampal $GABA_A$ receptors. I found that the serum antibodies #32 strongly reacted to the cells expressing β3 subunit alone and only slightly to those expressing γ2 subunit alone, but did not to those expressing α1, α2, α5 or β1 subunit alone (**Fig. 10*A***). Subsequent retrospective cell-based binding tests for the patients with LE showed that another patient (#17) had antibodies against the $GABA_A$ receptor α1/β3/γ2 and that the antibodies also strongly recognized β3 subunit (**Fig. 10*A***). I could not find any sera containing $GABA_A$ receptor (α1/β3/γ2) antibodies from patients with other immune-mediated disorders or neurodegenerative diseases and from healthy individuals (**Table2**).

Although both serum antibodies from the two patients did not bind to COS7 cells expressing α subunit alone, one may wonder whether the α subunit might not have been efficiently expressed at the cell surface without other subunits. To further examine the possible involvement of α subunit antibodies in the patient serum, COS7 cells were

transfected with various combinations of three subunit genes of the $GABA_A$ receptor, α1/β3/γ2, α1/β1/γ2, α2/β1/γ2 or α5/β1/γ2 (**Fig. 10*B***). There were no apparent differences in the slight binding of serum antibodies #32 to three different $GABA_A$ receptors, α1/β1/γ2, α2/β1/γ2 and α5/β1/γ2, indicating that the binding of serum antibodies was attributed to γ2 subunit, but neither to α1, α2, nor α5 subunits. The patient serum #17 did not show any apparent binding to α1/β1/γ2, α2/β1/γ2 or α5/β1/γ2. These results indicate that two patients with LE had autoantibodies directed against the $GABA_A$ receptor and that the extracellular part of β3 subunit was the main antigenic epitope recognized by the $GABA_A$ receptor antibodies. One of the two patients additionally had a low level of γ2 autoantibodies (patient #32), but both patients did not have any autoantibodies to α1, α2, α5 or β1 subunit.

2-3. $GABA_A$ receptor containing β3 subunit is the main target of the patient serum antibodies

I next asked whether the $GABA_A$ receptor is the main target of the patient antibodies. I took advantage of knockdown approach in cultured rat hippocampal neurons. MicroRNAs (miRNA-β3-211 and -347) for $GABA_A$ receptor β3 subunit were first validated by the reduced expression of exogenously expressed rat $GABA_A$ receptor β3 in HEK293T cells (**Fig. 11*A***). Then, by the cell-surface staining with anti-β2/β3 antibody I confirmed the efficient knockdown of β3 subunit in neurons (miR-β3-211) (**Fig. 11*B***). I noted that γ2 subunit clusters also disappeared in neurons in which β3 subunit was knocked down, confirming an essential role of β3 subunit in the $GABA_A$

receptor function in hippocampal neurons (DeLorey et al., 1998). Importantly, the overall immunoreactivity of the patient serum (#17 and #32) to the neurons in which β3 subunit was knocked down was mostly abolished (**Fig. 11*C***). These results demonstrate that the $GABA_A$ receptor containing β3 subunit is mainly targeted in these two patients with LE.

2-4. $GABA_A$ receptor autoantibodies reduce the number of both synaptic and surface $GABA_A$ receptors

Finally, I explored a mode of action of $GABA_A$ receptor autoantibodies. Previous studies showed that autoantibodies against NMDA and AMPA receptors induce the internalization of the corresponding receptors and reduce the number of synaptic receptors (Lai et al., 2009; Hughes et al., 2010). These previous findings inspired me to investigate whether $GABA_A$ receptor antibodies from patients with LE reduce the number of synaptic $GABA_A$ receptors. When hippocampal neurons were treated with the patient serum (#32) for 2 days, the number of synaptic $GABA_A$ receptor clusters, represented by γ2 or β3 subunit clusters colocalized with both gephyrin and vGAT, was significantly reduced (**Fig. 12*A***). Under the conditions, the number of surface γ2 subunit clusters representing both synaptic and extrasynaptic $GABA_A$ receptors was also heavily reduced. Importantly, the number of gephyrin clusters apposed to vGAT was also slightly reduced, suggesting that inhibitory synapses were secondarily decreased by the treatment with the serum antibodies (**Fig. 12*A***). This cell biological result was confirmed by the biochemical experiment: hippocampal neurons were treated with the patient serum #32 or control serum for 3 days and then the surface-expressed proteins

were labeled with biotin and purified by the avidin-conjugated beads (**Fig. 12*B***). In the patient serum-treated neurons, the amount of cell-surface $GABA_A$ receptor β3 subunit was significantly reduced and the total amount of β3 subunit tended to be reduced (but not significantly). This effect was specific to the $GABA_A$ receptor as the amount of the surface AMPA receptor subunit GluA1 and N-cadherin was not affected. Taken together, these results indicate that $GABA_A$ receptor autoantibodies cause a selective decrease in $GABA_A$ receptor surface density and synaptic localization, probably by enhancing the receptor internalization.

Discussion

Understanding a pathogenic mechanism for LGI1-mediated epilepsy represents an important goal of this study. For this purpose, I paid attention to the mode of action of LGI1 autoantibodies in LE. Previous studies showed that autoantibodies against NMDAR and AMPAR induce the internalization of the corresponding receptors and reduce the synaptic receptors (Lai et al., 2009; Hughes et al., 2010). Similar to MG and Lambert-Eaton syndrome, the functional downregulation of target ion channels has been a common mechanism of autoimmune encephalitis (*i.e.*, autoimmune channelopathies). In contrast, the mode of action of LGI1 antibodies shown here is unique in that antibodies neutralize the specific protein-protein interaction (between LGI1 and ADAM22/ADAM23). Because the genetic deletion of either LGI1, ADAM22 or ADAM23 causes lethal epilepsy in mouse models (Mitchell et al., 2001; Sagane et al., 2005; Owuor et al., 2009; Chabrol et al., 2010; Fukata et al., 2010; Yu et al., 2010) and because secretion-deficient LGI1 mutations occur in ADLTE (Senechal et al., 2005; Nobile et al., 2009), the reduced LGI1-ADAM22/23 interaction is the most reasonable pathogenic mechanism for LE characterized by seizures and amnesia.

This study strongly suggests that certain forms of inherited epilepsy and acquired seizures share the common mechanism that inhibition of the LGI1-ADAM22 interaction reduces synaptic AMPARs. How does LGI1 regulate synaptic AMPARs? AMPARs are anchored at the synapse through the interaction of their auxiliary subunit transmembrane AMPA receptor regulatory proteins (TARPs) with PSD-95 (Nicoll et al., 2006). This interaction is mediated through the PDZ1 or PDZ2 domain of PSD-95 (Elias and Nicoll, 2007), whereas ADAM22 binds to the PDZ3 domain-containing

region of PSD-95 (Fukata et al., 2006). Given that AMPARs and ADAM22 are anchored by the common PSD-95-scaffolding platform through different PDZ domains, it is speculated that the AMPAR/TARP can more stably bind to PSD-95 when LGI1/ADAM22 coincides (**Fig. 13**). Because Kv1.1 and Kv1.2 VGKC proteins also bind to the PDZ1 or PDZ2 domain of PSD-95 (Kim et al., 1995), and are indirectly associated with LGI1 through ADAM22 (Fukata et al., 2010), LGI1-ADAM22 interaction may similarly promote the Kv1 binding to PSD-95. Further structural and biochemical studies are required to address that LGI1-ADAM22 interaction regulates the scaffolding activity of PSD-95.

LGI1 has two domains, the LRR and EPTP repeat domains, and the EPTP repeat domain mediates the ADAM22/23 binding (Fukata et al., 2006). The epitope mapping showed that all the patient LGI1 autoantibodies tested were polyclonal antibodies recognizing both the LRR and EPTP repeat domains (Fig. 5*C*). In this study, I showed that LGI1 antibodies inhibit the interaction of LGI1 with ADAM22 by binding to the EPTP domain (Fig. 5*D*). Given that the LRR domain is frequently involved in the formation of protein-protein interaction (de Wit et al., 2011), it is suggested that LGI1 autoantibodies are involved in the pathogenesis of LE by binding to the LRR domain of LGI1 in addition to the EPTP domain. One possible candidate that may interact with the LRR domain of LGI1 is a Nogo receptor 1 (NgR1), which is a LRR domain-containing GPI-anchored protein. It has been recently reported that NgR1 functions as a receptor of LGI1 and facilitates LGI1 binding to ADAM22 (Thomas et al., 2010). Since the LRR domain can mediate the heteromeric LRR-LRR interaction (Bella et al., 2008), it may be worthwhile to investigate whether NgR1 binds to the LRR domain of LGI1, and if so,

whether LGI1 antibodies inhibit the binding of NgR1 to LGI1. Further studies are required to address this possibility.

In the course of screening for LGI1 antibodies, I additionally identified novel autoantibodies, including DCC, DPP10, ADAM23, CSMD1, ODZ1, TMEM132A, and $GABA_A$ receptor (Fig. 2*D*). Netrin-1 and DCC mediate axon-guidance during development. A recent study reported that the loss of DCC in the adult mouse brain results in the impaired memory (Horn et al., 2013). Taken together with the finding that newly identified DCC antibodies block the ligand/receptor interaction between Netrin-1 and DCC (Fig. 4*C*, *D*), DCC antibodies may modify clinical symptoms of LE. I also identified DPP10, an auxiliary subunit of Kv4.2, as a novel autoantigen in patients with NMT, LE, MoS, and encephalitis. Although I found that DPP10 always co-existed with DPP6 at similar levels in the immunoprecipitates from neurons (Fig. 1*B*), antibodies that directly bind to DPP6 or Kv4.2 were not detected in the sera (Fig. 2*C*), suggesting that DPP6 is physically associated with DPP10 in neurons. Given that DPP6, but not DPP10, was reported as a novel autoantigen of a protracted encephalitis with diarrhea (Boronat et al., 2013), DPP10 antibodies may be associated with similar clinical symptoms. Due to the limited number of patients in this study, I was unable to correlate the occurrence of DCC or DPP10 antibodies with specific diseases at this stage. However, it is noteworthy that DCC and DPP10 antibodies were significantly associated with specific features such as thymoma, myasthenia gravis, and neuromyotonia (Table 5). This study should serve as a prototype for future trials to clarify pathogenic roles of DCC and DPP10 antibodies in neuroimmunological disorders. Further assessment of individual serum antibodies and associated clinical

symptoms will reveal whether and how these novel autoantibodies are involved in the pathogenesis and phenotypic heterogeneity of LE and NMT.

I also found that the autoantibodies to $GABA_A$ receptors are associated with LE. The binding of the patient serum antibodies to the neuronal surface was mostly attributed to the $GABA_A$ receptor containing β3 subunit. $GABA_A$ receptor antibodies dramatically reduced the number of both synaptic and surface $GABA_A$ receptors. Thus, I first reveal a mode of action of $GABA_A$ receptor autoantibodies: down-regulation of the $GABA_A$ receptor function to cause abnormal neuronal excitation in the brain. Both two patients with LE and $GABA_A$ receptor antibodies had the antibodies directly targeting the β3 subunit. Based on the previous genetic studies that 1) mutations in $GABA_A$ receptor β3 cause genetic epilepsy syndromes (Macdonald et al., 2010) and that 2) the genetic loss of β3 subunit causes seizures and learning and memory deficits in mice (DeLorey et al., 1998), it is strongly suggested that the $GABA_A$ receptor antibodies directly cause the symptoms of LE such as seizures and memory impairment. Importantly, I found that patients with LE sometimes and patients with NMT very often have the autoantibodies against multiple targets (Fig 2*B* and 3*B*, *C*). In fact, one patient (#32) with $GABA_A$ receptor antibodies in this study was originally diagnosed as having malignant thymoma presented with the complications of myasthenia gravis (Miyazaki et al., 2012). After thymectomy, the patient developed generalized seizures with delirium and was diagnosed with paraneoplastic LE associated with the VGKC-complex antibodies (649 pM, positive > 400 pM) [i.e., suspected of having LGI1 and/or CASPR2 antibodies (Irani et al., 2010; Lai et al., 2010)]. By my established cell-based ELISA test, I found that this patient had the minimum level of LGI1 antibodies but did not have CASPR2

antibodies (Table 2). Another patient (#17) also had invasive thymoma and the VGKC-complex antibodies (403 pM) at onset of LE (Ohshita et al., 2006). I found that the patient serum contained only the minimum level of CASPR2 autoantibodies (Table 2). Taking into account the data that the knockdown of $GABA_A$ receptor β3 subunit greatly reduced the serum reactivity to neurons (Fig. 11*C*), it is likely that seizures or cognitive dysfunction observed in these patients could be mainly attributed to the $GABA_A$ receptor dysfunction. Importantly, both cases showed the similar brain MRI finding, extensive lesions involving bilateral temporal lobes (Ohshita et al., 2006; Miyazaki et al., 2012). Because LE with LGI1 autoantibodies is featured by the typical MRI finding with the focal lesion of medial temporal lobes (Cash et al., 2011; Lancaster et al., 2011a), encephalitis associated with the $GABA_A$ receptor antibodies may be distinguished as a different class of autoimmune encephalitis.

Finally, this study establishes that LGI1 autoantibodies specifically cause LE through inhibiting the ligand-receptor interaction between LGI1 and ADAM22 that controls AMPAR function (**Fig. 13**). "Blocking the ligand-receptor interaction" is a novel mode of autoantibody-mediated pathogenesis for encephalitis/LE, different from a previous concept "autoimmune channelopathy". This is akin to inherited epilepsy with LGI1 mutations, whose pathogenesis cannot be explained by a common "channelopathy" concept. Thus, this study should provide insights into the molecular basis of genetic and acquired epileptic disorders with LGI1 dysfunction, and contribute to understanding the mechanisms for regulating brain excitability and memory storage in human.

Abbreviations

ADAM	A disintegrin and metalloprotease domain
ADLTE	Autosomal dominant lateral temporal lobe epilepsy
ALS	Amyotrophic lateral sclerosis
AMPA	α-amino-3-hydroxy-5-methyl-4-isoxazolepropionic acid
AMPAR	AMPA receptor
BSA	Bovine serum albumin
cDNA	Complementary DNA
CNS	Central nervous system
COS	CV-1 in Origin, and carrying the SV40 genetic material
CSMD1	Cub and sushi multiple domains 1
DCC	Deleted in colorectal carcinoma
DIV	Days in vitro
DMEM	Dulbecco's modified Eagle's minimal essential medium
DPP10	Dipeptidyl-peptidase 10
EPTP	Epitempin
GABA	γ-aminobutyric acid
HA	Hemagglutinin
HEK293	Human embryonic kidney 293
i.e.	id est
IF	Immunofluorescence
IgG	immunoglobulin
IP	Immunoprecipitation
KO	Knockout

LC	Liquid chromatography
LE	Limbic encephalitis
LGI1	Leucine-rich, glioma inactivated 1
LRR	Leucine-rich repeat
MG	Myasthenia gravis
MoS	Morvan syndrome
MS	Mass spectrometry
MSA	Multiple system atrophy
NgR1	Nogo receptor 1
NMDAR	NMDA receptor
NMT	Neuromyotonia
ODZ1/4	Odd Oz/ten-m homolog 1/4
PBS	Phosphate buffered saline
STED	Stimulated emission depletion
SCD	Spinocerebellar degeneration
TARP	Transmembrane AMPA receptor regulatory protein
TMEM132A	Transmembrane protein 132A
vGAT	Vesicular GABA transporter
vGluT	Vesicular glutamate transporter
VGKC	Voltage-gated potassium channel
WT	Wild type

References

Acsády L, Kamondi A, Sík A, Freund T, Buzsáki G. 1998. GABAergic cells are the major postsynaptic targets of mossy fibers in the rat hippocampus. *J Neurosci* 18: 3386-3403

Bella J, Hindle KL, McEwan PA, Lovell SC. 2008. The leucine-rich repeat structure. *Cell Mol Life Sci* 65: 2307-2333

Boronat A, Gelfand JM, Gresa-Arribas N, Jeong HY, Walsh M, et al. 2013. Encephalitis and antibodies to dipeptidyl-peptidase-like protein-6, a subunit of Kv4.2 potassium channels. *Ann Neurol* 73: 120-128

Cash SS, Larvie M, Dalmau J. 2011. Case records of the Massachusetts General Hospital. Case 34-2011: A 75-year-old man with memory loss and partial seizures. *N Engl J Med* 365: 1825-1833

Chabrol E, Navarro V, Provenzano G, Cohen I, Dinocourt C, et al. 2010. Electroclinical characterization of epileptic seizures in leucine-rich, glioma-inactivated 1-deficient mice. *Brain* 133: 2749-2762

Dalmau J, Gleichman AJ, Hughes EG, Rossi JE, Peng X, et al. 2008. Anti-NMDA-receptor encephalitis: case series and analysis of the effects of antibodies. *Lancet Neurol* 7: 1091-1098

DeLorey TM, Handforth A, Anagnostaras SG, Homanics GE, Minassian BA, et al. 1998. Mice lacking the beta3 subunit of the $GABA_A$ receptor have the epilepsy phenotype and

many of the behavioral characteristics of Angelman syndrome. *J Neurosci* 18: 8505-8514

Elias GM, Nicoll RA. 2007. Synaptic trafficking of glutamate receptors by MAGUK scaffolding proteins. *Trends Cell Biol* 17: 343-352

Fang C, Deng L, Keller CA, Fukata M, Fukata Y, et al. 2006. GODZ-mediated palmitoylation of $GABA_A$ receptors is required for normal assembly and function of GABAergic inhibitory synapses. *J Neurosci* 26: 12758-12768

Fukata Y, Adesnik H, Iwanaga T, Bredt DS, Nicoll RA, Fukata M. 2006. Epilepsy-related ligand/receptor complex LGI1 and ADAM22 regulate synaptic transmission. *Science* 313: 1792-1795

Fukata Y, Dimitrov A, Boncompain G, Vielemeyer O, Perez F, Fukata M. 2013. Local palmitoylation cycles define activity-regulated postsynaptic subdomains. *J Cell Biol* 202: 145-161

Fukata Y, Lovero KL, Iwanaga T, Watanabe A, Yokoi N, et al. 2010. Disruption of LGI1-linked synaptic complex causes abnormal synaptic transmission and epilepsy. *Proc Natl Acad Sci USA* 107: 3799-3804

Gu W, Brodtkorb E, Steinlein OK. 2002. LGI1 is mutated in familial temporal lobe epilepsy characterized by aphasic seizures. *Ann Neurol* 52: 364-367

Horn KE, Glasgow SD, Gobert D, Bull SJ, Luk T, et al. 2013. DCC expression by neurons regulates synaptic plasticity in the adult brain. *Cell Rep* 3: 173-185

Hughes EG, Peng X, Gleichman AJ, Lai M, Zhou L, et al. 2010. Cellular and synaptic mechanisms of anti-NMDA receptor encephalitis. *J Neurosci* 30: 5866-5875

Irani SR, Alexander S, Waters P, Kleopa KA, Pettingill P, et al. 2010. Antibodies to Kv1 potassium channel-complex proteins leucine-rich, glioma inactivated 1 protein and contactin-associated protein-2 in limbic encephalitis, Morvan's syndrome and acquired neuromyotonia. *Brain* 133: 2734-2748

Irani SR, Pettingill P, Kleopa KA, Schiza N, Waters P, et al. 2012. Morvan syndrome: Clinical and serological observations in 29 cases. *Ann Neurol* 72: 241-255

Kalachikov S, Evgrafov O, Ross B, Winawer M, Barker-Cummings C, et al. 2002. Mutations in LGI1 cause autosomal-dominant partial epilepsy with auditory features. *Nat Genet* 30: 335-341

Kegel L, Aunin E, Meijer DN, Bermingham Jr JR. 2013. LGI proteins in the nervous system. *ASN Neuro* 5: 167-181

Kim E, Niethammer M, Rothschild A, Jan YN, Sheng M. 1995. Clustering of Shaker-type K^+ channels by interaction with a family of membrane-associated guanylate kinases. *Nature* 378: 85-88

Kleopa KA, Elman LB, Lang B, Vincent A, Scherer SS. 2006. Neuromyotonia and limbic encephalitis sera target mature Shaker-type K^+ channels: subunit specificity correlates with clinical manifestations. *Brain* 129: 1570-1584

Lai HC, Jan LY. 2006. The distribution and targeting of neuronal voltage-gated ion channels. *Nat Rev Neurosci* 7: 548-562

Lai M, Hughes EG, Peng X, Zhou L, Gleichman AJ, et al. 2009. AMPA receptor antibodies in limbic encephalitis alter synaptic receptor location. *Ann Neurol* 65: 424-434

Lai M, Huijbers MG, Lancaster E, Graus F, Bataller L, et al. 2010. Investigation of LGI1 as the antigen in limbic encephalitis previously attributed to potassium channels: a case series. *Lancet Neurol* 9: 776-785

Lancaster E, Dalmau J. 2012. Neuronal autoantigens--pathogenesis, associated disorders and antibody testing. *Nat Rev Neurol* 8: 380-390

Lancaster E, Martinez-Hernandez E, Dalmau J. 2011. Encephalitis and antibodies to synaptic and neuronal cell surface proteins. *Neurology* 77: 179-189

Macdonald RL, Kang JQ, Gallagher MJ. 2010. Mutations in $GABA_A$ receptor subunits associated with genetic epilepsies. *J Physiol* 588: 1861-1869

Mitchell KJ, Pinson KI, Kelly OG, Brennan J, Zupicich J, et al. 2001. Functional analysis of secreted and transmembrane proteins critical to mouse development. *Nat Genet* 28: 241-249

Miyazaki T, Fukaya M, Shimizu H, Watanabe M. 2003. Subtype switching of vesicular glutamate transporters at parallel fibre-Purkinje cell synapses in developing mouse cerebellum. *Eur J Neurosci* 17: 2563-2572

Miyazaki Y, Hirayama M, Watanabe H, Usami N, Yokoi K, et al. 2012. Paraneoplastic encephalitis associated with myasthenia gravis and malignant thymoma. *J Clin Neurosci* 19: 336-338

Morante-Redolat JM, Gorostidi-Pagola A, Piquer-Sirerol S, Saenz A, Poza JJ, et al. 2002. Mutations in the LGI1/Epitempin gene on 10q24 cause autosomal dominant lateral temporal epilepsy. *Hum Mol Genet* 11: 1119-1128

Nicoll RA, Tomita S, Bredt DS. 2006. Auxiliary subunits assist AMPA-type glutamate receptors. *Science* 311: 1253-1256

Nobile C, Michelucci R, Andreazza S, Pasini E, Tosatto SC, Striano P. 2009. LGI1 mutations in autosomal dominant and sporadic lateral temporal epilepsy. *Hum mutat* 30: 530-536

Noebels JL. 2003. The biology of epilepsy genes. *Annu Rev Neurosci* 26: 599-625

Oh-hashi K, Imai K, Koga H, Hirata Y, Kiuchi K. 2010. Knockdown of transmembrane protein 132A by RNA interference facilitates serum starvation-induced cell death in Neuro2a cells. *Mol Cell Biochem* 342: 117-123

Ohshita T, Kawakami H, Maruyama H, Kohriyama T, Arimura K, Matsumoto M. 2006. Voltage-gated potassium channel antibodies associated limbic encephalitis in a patient with invasive thymoma. *J Neurol Sci* 250: 167-169

Owuor K, Harel NY, Englot DC, Hisama F, Blumenfeld H, Strittmatter SM. 2009. LGI1-associated epilepsy through altered ADAM23-dependent neuronal morphology. *Mol Cell Neurosci* 42: 448-457

Poliak S, Gollan L, Martinez R, Custer A, Einheber S, et al. 1999. Caspr2, a new member of the neurexin superfamily, is localized at the juxtaparanodes of myelinated axons and associates with K^+ channels. *Neuron* 24: 1037-1047

Ripke S, Sanders AR, Kendler KS, Levinson DF, Sklar P, et al. 2011. Genome-wide association study identifies five new schizophrenia loci. *Nat Genet* 43: 969-976

Sagane K, Hayakawa K, Kai J, Hirohashi T, Takahashi E, et al. 2005. Ataxia and peripheral nerve hypomyelination in ADAM22-deficient mice. *BMC Neurosci* 6: 33

Schulte U, Thumfart JO, Klocker N, Sailer CA, Bildl W, et al. 2006. The epilepsy-linked lgi1 protein assembles into presynaptic kv1 channels and inhibits inactivation by kvβ1. *Neuron* 49: 697-706

Senechal KR, Thaller C, Noebels JL. 2005. ADPEAF mutations reduce levels of secreted LGI1, a putative tumor suppressor protein linked to epilepsy. *Hum Mol Genet* 14: 1613-1620

Steinlein OK. 2004. Genetic mechanisms that underlie epilepsy. *Nat Rev Neurosci* 5: 400-408

Thomas R, Favell K, Morante-Redolat J, Pool M, Kent C, et al. 2010. LGI1 is a Nogo receptor 1 ligand that antagonizes myelin-based growth inhibition. *J Neurosci* 30: 6607-6612

Vincent A, Lang B, Kleopa KA. 2006. Autoimmune channelopathies and related neurological disorders. *Neuron* 52: 123-138

Watanabe M, Fukaya M, Sakimura K, Manabe T, Mishina M, Inoue Y. 1998. Selective scarcity of NMDA receptor channel subunits in the stratum lucidum (mossy fibre-recipient layer) of the mouse hippocampal CA3 subfield. *Eur J Neurosci* 10: 478-487

Yamasaki M, Matsui M, Watanabe M. 2010. Preferential localization of muscarinic M1 receptor on dendritic shaft and spine of cortical pyramidal cells and its anatomical evidence for volume transmission. *J Neurosci* 30: 4408-4418

Yamasaki M, Miyazaki T, Azechi H, Abe M, Natsume R, et al. 2011. Glutamate receptor delta2 is essential for input pathway-dependent regulation of synaptic AMPAR contents in cerebellar Purkinje cells. *J Neurosci* 31: 3362-3374

Yamazaki M, Fukaya M, Hashimoto K, Yamasaki M, Tsujita M, et al. 2010. TARPs gamma-2 and gamma-7 are essential for AMPA receptor expression in the cerebellum. *Eur J Neurosci* 31: 2204-2220

Yu YE, Wen L, Silva J, Li Z, Head K, et al. 2010. Lgi1 null mutant mice exhibit myoclonic seizures and CA1 neuronal hyperexcitability. *Hum Mol Genet* 19: 1702-1711

Zhang JH, Chung TD, Oldenburg KR. 1999. A Simple Statistical Parameter for Use in Evaluation and Validation of High Throughput Screening Assays. *J Biomol Screen* 4: 67-73

Zhou YD, Lee S, Jin Z, Wright M, Smith SE, Anderson MP. 2009. Arrested maturation of excitatory synapses in autosomal dominant lateral temporal lobe epilepsy. *Nat Med* 15: 1208-1214

Table 1. Clinical features in 145 patients tested in this study

	VGKC-Ab (≥400 pM) n=69			VGKC-Ab (<400 pM) n=76		
	LE (n=39)	**NMT/MoS (n=19/2)**	**Others* (n=9)**	**LE (n=20)**	**NMT/MoS (n=14/0)**	**Others* (n=42)**
Age (range)	58 (6-82)	52 (1-78)	38 (1-70)	48 (21-82)	39 (21-85)	41 (3-84)
Male : Female	18 : 21	15 : 6	4 : 5	8 : 12	7 : 7	26 : 16
Memory loss	36	2	3	16	0	20
Confusion	35	2	4	18	0	23
Seizures‡	28	1	4	12	0	17
Neuromyotonia‡	2	20	1	0	14	5
MRI medial temporal high signal on T2 or FLAIR‡	31	1	0	13	0	5
Hyponatremia‡	20	1	0	5	0	6
Movement disorders§	8	1	2	1	0	7
Active tumor‡	10	7	1	0	1	5
Any dysautonomia¶	8	7	1	1	6	4
VGKC-Ab titer (pM) (range)	895 (407-2493)	780 (426-2593)	561 (400-741)	49 (0-384)	93 (71-384)	13 (0-386)

The data represent the number or median (range). *Patients with Others; see Materials and Methods. LE=limbic encephalitis. NMT=neuromyotonia. MoS=Morvan syndrome. MG=myasthenia gravis. ‡Data available for 144 patients. §Data available for 124 patients. ¶Data available for 130 patients.

Table 2. All serum data utilized in this study

																	> 0.8	> 0.8	> 0.8	> 0.8	
																	0.5 <_ < 0.8	0.3 <_ < 0.8	0.3 <_ < 0.8	0.4 <_ < 0.8	
serum#	Diagnosis in this study	Original diagnosis	VGKC-Ab titer (pM)	Cell-surface staining of HP neuron and immunoprecipitation		Cell-based binding assay											ELISA (relative absorbance)				serum#
				HP binding	Proteins identified in LC-MS/MS analysis	LGI1-GPI	CASPR2	DCC	DPP10	$GABA_AR$**	ADAM22	ADAM23	LRR3-EPTP1	LRR1	LGI4/ADAM22		LGI1	CASPR2	DCC	DPP10	
1	NMT	acquired neuromyotonia	2593	++	CASPR2	+	+	+	-	-	-	-	+	+	-		0.52	1.42	0.44	0.27	1
2	LE	VGKC-LE	2258	++	LGI1, ADAM11, ADAM23, PSD-95	+	-	+	-	-	-	-	+	+	-		1.68	-0.07	0.32	0.17	2
3	LE	VGKC-LE	1794	+	(LGI1)*	+	-	+	-	-	-	-	+	+	-		1.11	0.28	0.82	0.09	3
4	LE	VGKC-LE	1682	+	LGI1	+	-	-	-	-	-	-	+	+	-		1.60	0.11	0.12	0.14	4
5	NMT	acquired neuromyotonia	1584	+	LGI1	+	-	-	-	-	-	-	+	+	-		0.99	0.08	0.23	0.17	5
6	NMT	acquired neuromyotonia	1576	++	DCC, CASPR2, LGI1	+	+	+	-	-	-	-	+	+	-		0.59	0.67	1.60	0.02	6
7	LE	VGKC-LE	1510	++	LGI1	+	+	-	-	-	-	-	+	+	-		0.18†	0.12†	-0.16	0.00	7
8	LE	VGKC-LE	1497	+	(LGI1)*	+	-	-	-	-	-	-	+	+	-		1.33	0.10	0.11	0.18	8
9	LE	VGKC-LE	1450	++	CASPR2, ODZ1/4, CSMD1, LGI1, ADAM23	+	+	+	-	-	-	-	+	+	-		1.08	0.85	0.27†	0.08	9
10	LE	VGKC-LE	1332	-		+	-	+	-	-	-	-	+	+	-		1.64	-0.13	0.19†	0.04	10
11	LE	VGKC-LE	1221	+	(LGI1)*	+	-	+	-	-	-	-	+	+	-		0.86	-0.03	0.11†	0.08	11
12	LE	VGKC-LE	1138	++	LGI1, ADAM11	+	-	-	-	-	-	-	+	+	-		1.26	0.19	0.06	0.22	12
13	LE	VGKC-LE	1136	-		+	-	-	-	-	-	-	+	+	-		1.48	0.25	0.08	0.34	13
14	NMT	acquired neuromyotonia	1136	-		-	-	-	-	-	-	-			-		0.45	-0.11	0.09	0.25	14
15	LE	VGKC-LE	1105	++	ADAM11, PSD-95, (LGI1)*	+	-	-	-	-	-	-	+	+	-		1.69	0.08	0.12	0.07	15
16	LE	VGKC-LE suspected	947	-		-	-	-	-	-	-	-			-		0.15	0.03	0.09	0.24	16
17	LE	VGKC-LE	895	++	CASPR2, DCC	-	+	+	-	+	-	-			-		0.07	0.43	0.43	-0.09	17
18	MoS	Morvan's syndrome	893	-		+	+	+	+	-	-	-	+	+	-		0.81	0.31	1.17	0.58	18
19	LE	VGKC-LE	890	-		+	-	-	-	-	-	-	+	+	-		1.15	0.14	-0.02	0.15	19
20	MoS	Morvan's syndrome	863	-		-	-	-	-	-	-	-			-		0.07	0.05	0.18	-0.04	20
21	NMT	acquired neuromyotonia	822	++	CASPR2, DCC	+	+	+	-	-	-	-	+	+	-		0.87	0.62	1.37	-0.13	21
22	LE	VGKC-LE	809	-		+	-	-	-	-	-	-	+	+	-		1.48	0.05	0.04	0.01	22
24	NMT	acquired neuromyotonia	784	++	DCC, DPP10, DPP6	+	+	+	+	-	-	-	+	+	-		0.45†	0.18†	0.70	0.48	24
25	NMT	acquired neuromyotonia	780	-		-	-	-	-	-	-	-			-		0.33	0.10	0.10	0.15	25
26	Others	NMDAR encephalits	741	+	n.d.	-	-	-	-	-	-	-			-		0.21	0.04	0.00	-0.05	26
27	LE	VGKC-LE	729	++	CASPR2, DPP10, DPP6, (LGI1)*	+	+	-	+	-	-	+	+	+	-		0.25†	1.99	0.11	1.02	27
28	NMT	acquired neuromyotonia	716	+	(LGI1)*	+	+	+	-	-	-	-	+	+	-		0.88	0.78	0.69	0.01	28
29	NMT	acquired neuromyotonia	714	-		-	-	-	-	-	-	-			-		0.08	-0.10	-0.18	0.01	29
30	LE	VGKC-LE	660	-		+	-	-	-	-	-	-	+	+	-		1.29	0.16	0.18	0.02	30
31	LE	VGKC-LE	654	-		+	-	-	-	-	-	-	+	+	-		1.57	0.06	0.24	-0.01	31
32	LE	VGKC-LE	649	++	$GABA_AR$ α1, (LGI1)*	+	-	+	-	+	-	-	+	+	-		0.54	-0.06	0.46	0.10	32
33	Others	encephalitis (post-infectious)	615	-		-	-	-	-	-	-	-			-		0.15	0.01	-0.03	0.03	33
34	LE	VGKC-LE	594	-		+	-	-	-	-	-	-	+	+	-		2.02	0.12	0.06	0.06	34
35	LE	VGKC-LE	588	+	LGI1	+	-	-	-	-	-	-	+	+	-		1.01	0.22	-0.03	0.07	35
36	LE	VGKC-LE	585	-		+	-	-	-	-	-	-	+	+	-		1.76	0.04	0.05	0.02	36
37	Others	encephalopathy (paraneoplastic syndrome)	561	-		-	-	-	-	-	-	-			-		0.17	-0.04	0.14	-0.04	37
38	LE	VGKC-LE suspected	559	+	n.d.	-	-	-	-	-	-	-			-		0.06	-0.03	0.04	0.01	38
39	LE	VGKC-LE	554	-		+	-	-	-	-	-	-	+	+	-		1.73	0.00	-0.16	0.07	39
40	LE	VGKC-LE suspected	532	+	GluA1, GluA2	-	-	-	-	-	-	-					0.10	0.05	-0.01	0.09	40
41	LE	VGKC-LE	518	-		+	-	+	-	-	-	-	+	+			0.82	0.17	0.15†	-0.07	41
42	LE	limbic encephalitis (unknown etiology)	448	-		-	-	-	-	-	-	-					0.30	-0.07	-0.03	0.13	42
43	LE	VGKC-LE	446	-		+	-	-	-	-	-	-	+	+			1.80	-0.05	-0.06	0.06	43
44	NMT	acquired neuromyotonia	426	-		-	-	-	-	-	-	-					-0.33	0.13	-0.07	0.14	44
45	LE	limbic encephalitis (unknown etiology)	419	-		-	-	-	-	-	-	-					0.25	0.20	0.04	0.21	45
46	Others	Hashimoto's encephalopathy	415	-		-	-	-	-	-	-	-					0.20	0.07	-0.07	-0.02	46
48	Others	cramp-fasciculation syndrome	400	-		-	-	-	-	-	-	-					0.19	0.06	-0.02	0.03	48
50	LE	VGKC-LE	384	-		+	-	-	-	-	-	-	+	+			1.19	-0.04	-0.13	-0.02	50
51	NMT	acquired neuromyotonia	384	-		-	-	-	-	-	-	-					0.09	0.19	0.00	0.11	51
52	NMT	acquired neuromyotonia	373	-		+	-	-	-	-	-	-	+	+			0.82	0.03	-0.11	0.18	52
53	Others	encephalitis (unknown etiology)	355	++	GluA1, GluA2, GluA4	-	-	-	-	-	-	-					0.01	0.02	0.07	0.11	53
54	NMT	acquired neuromyotonia	334	-		-	-	-	-	-	-	-					0.12	0.05	0.13	0.02	54
55	Others	encephalitis (unknown etiology)	332	-		-	-	+	-	-	-	-					0.22	0.09	0.13†	0.13	55
56	LE	limbic encephalitis (unknown etiology)	315	++	GluA1, GluA2, GluA3, GluA4	-	-	-	-	-	-	-					0.02	0.13	0.09	0.12	56
57	Others	post-encephalitis (unknown etiology)	305	+	n.d.	-	-	-	-	-	-	-					0.11	0.20	0.14	0.04	57
58	Others	encephalopathy (unknown etiology)	220	-		-	-	-	-	-	-	-					0.57‡	-0.05	-0.04	-0.12	58
59	NMT	acquired neuromyotonia	206	+	n.d.	-	-	-	-	-	-	-					0.42	0.22	0.01	0.05	59
61	Others	NMDAR encephalitis	0	+		-	-	-	-	-							0.14	-0.02	0.02	0.12	61
63	NMT	acquired neuromyotonia	1800	++	DCC, (LGI1)*	+	+	+	-	-							0.50	0.71	0.09†	0.03	63
64	LE	VGKC-LE	1339	++	TMEM132A, LGI1	+	-	-	-	-							0.88	0.21	0.16	-0.01	64
65	LE	VGKC-LE	1266	+	LGI1	+	-	-	-	-							1.61	0.25	0.03	-0.07	65
66	LE	VGKC-LE	1101	+	(LGI1)*	+	-	-	-	-							1.11	0.03	0.17	-0.08	66
67	LE	VGKC-LE suspected	875	-					-	-							-0.11	0.07	-0.15	-0.12	67

68	NMT	acquired neuromyotonia	731	-					-	-						0.26	0.16	0.03	0.01	68
69	NMT	acquired neuromyotonia	698	-					-	-						0.38	0.14	-0.21	-0.02	69
70	Others	intractable epilepsy	574	+	n.d.	-	-	-	-	-						0.35	0.08	0.11	-0.13	70
71	Others	Hashimoto's encephalopathy suspected	521	-						-						0.05	0.02	-0.17	-0.35	71
72	NMT	acquired neuromyotonia	438	++	DPP10, DPP6, (LGI1)*	+	+	+	+	-						0.68	0.31	0.65	1.02	72
73	NMT	acquired neuromyotonia	436	-						-						0.15	-0.02	0.14	0.03	73
74	Others	intractable epilepsy	409	+	n.d.	-				-						0.61[1]	0.17	0.26	0.05	74
75	LE	limbic encephalitis (unknown etiology)	247	-						-						0.02	0.14	0.16	-0.05	75
76	Others	encephalitis (unknown etiology)	188	-						-						0.01	0.00	0.17	-0.04	76
78	Others	encephalitis (unknown etiology)	43	++	GluA1, GluA2, GluA3, DPP10, DPP6	-	-	-	+	-						0.29	0.29	0.16	0.90	78
79	Others	encephalitis (unknown etiology)	0	-						-						0.26	-0.02	-0.03	0.03	79
80	LE	limbic encephalitis (unknown etiology)	0	-						-						0.29	0.14	0.06	0.09	80
81	Others	NMDAR encephalitis suspected	0	-						-						0.19	-0.22	-0.18	-0.17	81
82	LE	limbic encephalitis (unknown etiology)	0	-						-						-0.04	0.02	0.05	0.01	82
83	Others	autoimmune encephalitis suspected	0	-						-						0.29	-0.17	-0.15	0.00	83
84	Others	autoimmune encephalitis suspected	0	+	n.d.	-	-	-	-	-						0.06	0.18	-0.03	0.24	84
85	LE	limbic encephalitis (unknown etiology)	0	++	n.d.	-	-	-	-	-						0.09	0.22	-0.02	0.04	85
87	Others	encephalitis (post-infectious)	0	-						-						0.05	-0.02	-0.25	0.13	87
89	NMT	acquired neuromyotonia	0	-						-						0.43	0.12	0.17	0.06	89
90	NMT	acquired neuromyotonia	276	-						-						0.30	0.26	0.22	-0.03	90
91	NMT	acquired neuromyotonia	146	-						-						0.06	0.12	0.16	0.08	91
92	NMT	acquired neuromyotonia	106	-						-						0.09	0.11	0.07	-0.13	92
93	NMT	acquired neuromyotonia	180	-						-						0.16	0.07	0.10	0.11	93
94	NMT	acquired neuromyotonia	105	-						-						0.22	0.09	0.11	0.30	94
95	NMT	acquired neuromyotonia	112	-						-						0.24	0.04	0.00	0.13	95
96	NMT	acquired neuromyotonia	176	-						-						0.10	0.04	0.14	0.19	96
98	Others	encephalopathy	237	-						-						-0.07	0.15	0.03	0.14	98
99	LE	limbic encephalitis (unknown etiology)	233	-						-						-0.15	0.13	-0.02	-0.07	99
100	LE	limbic encephalitis (unknown etiology)	191	-						-						0.30	0.06	-0.23	0.02	100
101	LE	limbic encephalitis (unknown etiology)	146	-						-						0.09	0.10	0.08	0.02	101
102	LE	limbic encephalitis (unknown etiology)	142	-						-						-0.19	0.03	0.09	0.00	102
103	Others	Hashimoto's encephalopathy suspected	124	-						-						-0.17	0.10	-0.02	-0.04	103
104	Others	mengitis (unknown etiology)	114	-						-						0.17	0.00	0.07	-0.19	104
105	LE	limbic encephalitis (unknown etiology)	112	-						-						-0.12	-0.03	0.14	-0.03	105
106	LE	limbic encephalitis (unknown etiology)	92	-						-						0.10	-0.01	0.05	0.05	106
107	LE	limbic encephalitis (unknown etiology)	61	-						-						-0.07	0.21	0.13	0.12	107
108	Others	cramp-fasciculation syndrome suspected	60	-						-						-0.07	0.14	0.01	0.05	108
109	Others	meningitis	41	-						-						-0.15	0.12	-0.12	0.01	109
110	LE	limbic encephalitis (unknown etiology)	36	++	n.d.	-	-	-	-	-						-0.07	-0.01	0.00	0.05	110
112	LE	limbic encephalitis (unknown etiology)	0	-						-						0.14	0.01	0.12	0.03	112
113	Others	post brain stem encephalitis	0	-						-						0.01	0.00	0.03	-0.01	113
115	LE	limbic encephalitis (unknown etiology)	0	-						-						0.40	-0.05	0.05	0.12	115
117	LE	limbic encephalitis (unknown etiology)	0	-						-						0.25	0.15	-0.01	0.13	117
118	Others	medial temporal sclerosis	0	-						-						0.15	0.23	-0.04	0.12	118
119	Others	medial temporal sclerosis	0	-						-						0.24	-0.03	0.05	0.02	119
120	Others	cramp-fasciculation syndrome suspected	0	-						-						0.07	0.01	0.10	0.04	120
121	LE	limbic encephalitis (unknown etiology)	0	-						-						0.27	0.03	-0.04	-0.01	121
122	LE	limbic encephalitis (unknown etiology)	0	-						-						0.01	0.21	0.09	-0.08	122
123	LE	limbic encephalitis (unknown etiology)	0	-						-						0.16	0.10	0.05	0.05	123
124	Others	stiff-person syndrome	0	-						-						0.38	0.19	0.17	0.02	124
125	Others	encephalitis (cerebellitis)	0	-						-						0.18	0.01	0.01	0.24	125
126	Others	cramp-fasciculation syndrome suspected	0	-						-						0.09	0.12	0.06	0.15	126
127	Others	meningitis	0	-						-						0.14	0.05	0.06	0.10	127
128	Others	epilepsy	0	-						-						0.16	0.12	-0.03	0.04	128
129	Others	epilepsy	0	-						-						-0.04	0.07	0.14	0.10	129
130	Others	cramp-fasciculation syndrome suspected	0	-		-				-						0.50[1]	0.10	0.10	0.15	130
131	Others	encephalitis (unknown etiology)	0	-						-						0.00	-0.04	-0.07	0.27	131
132	Others	encephalopathy (mitochondrial suspected)	0	-						-						0.08	-0.06	-0.07	0.17	132
133	Others	encephalitis (unknown etiology)	0	++	GluA1, GluA2, GluA4	-	-	-	-	-						0.10	0.03	0.17	-0.06	133
134	Others	encephalopathy (associated with GluR Abs)	0	-						-						0.10	0.00	0.13	0.08	134
135	Others	encephalopathy (associated with GluR Abs)	25.5	-						-						0.25	0.12	0.07	-0.16	135
136	LE	VGKC-LE	1903	++	LGI1	+	-	-	-	-						1.50	-0.09	0.07	-0.07	136
137	LE	VGKC-LE	517	+	n.d.	+				-						1.32	-0.02	0.10	0.13	137
138	Others	encephalitis (unknown etiology)	367	-						-						0.07	0.16	0.14	-0.12	138
139	Others	encephalitis (herpetic suspected)	358	-						-						0.26	0.00	0.01	0.18	139
140	Others	encephalopathy (paraneoplastic syndrome)	259	-						-						0.36	0.01	0.05	-0.06	140

141	NMT	acquired neuromyotonia	239	+	n.d.	+	+			-						0.66	0.37	0.12	0.04	141
142	Others	NMDAR encephalits suspected	153	-						-						0.27	0.00	0.06	0.09	142
143	Others	encephalopathy	149	-						-						0.10	-0.02	0.07	-0.04	143
144	Others	myasthenia gravis (with invasive thymoma)	138	++	DCC	-	-	+		-						0.14	0.14	1.59	-0.09	144
146	Others	autoimmune encephalitis suspected	83	-						-						0.24	0.15	-0.01	-0.01	146
147	NMT	acquired neuromyotonia	71	-						-						-0.03	0.14	-0.02	0.12	147
148	LE	VGKC-LE	2493	++	LGI1, Kvβ2	+	-	-	-	-						1.89	0.12	0.06	-0.03	148
149	LE	VGKC-LE	1711	++	LGI1	+	-	-	-	-						1.25	0.05	0.05	0.03	149
150	NMT	acquired neuromyotonia	563	-						-						0.12	0.11	0.13	0.00	150
152	LE	VGKC-LE	407.1	-		-	-	-	-	-						0.00	0.01	0.16	0.02	152
153	Others	cramp-fasciculation syndrome	290.7	-						-						0.20	0.24	0.10	0.10	153
154	NMT	acquired neuromyotonia	808.8	++	CASPR2, GAD65	+	+	-	-	-						0.56	0.54	0.02	-0.12	154
155	Others	myasthenia gravis	715.7	-		-	-	-	-	-						0.08	-0.03	0.10	-0.02	155
159	Others	intractable epilepsy	386.3	-		-	-	-	-	-						0.12	0.07	0.19	0.02	159
160	NMT	acquired neuromyotonia	456.4	++	GluN3B	-	-	-	-	-						0.14	0.00	0.09	-0.06	160
161	LE	VGKC-LE	2121.4	++	LGI1	+	-	-	-	-						1.86	0.16	0.10	-0.17	161
162	NMT	acquired neuromyotonia	194	-		-	-	-	-	-						0.11	0.04	0.10	0.00	162
Contr #1	disease control	ALS								-						-0.34	0.03	0.06	-0.04	Contr #1
Contr #2	disease control	ALS								-						0.09	0.05	0.00	-0.31	Contr #2
Contr #3	disease control	CBD								-						-0.14	0.20	-0.05	0.05	Contr #3
Contr #4	disease control	SCD								-						0.01	-0.09	0.05	0.14	Contr #4
Contr #5	disease control	ALS								-						-0.05	-0.01	0.15	0.07	Contr #5
Contr #6	disease control	ALS								-						-0.04	0.06	0.08	0.06	Contr #6
Contr #7	disease control	PD								-						0.03	-0.01	0.09	0.02	Contr #7
Contr #8	disease control	ALS								-						0.01	0.06	0.00	0.10	Contr #8
Contr #9	disease control	SCD								-						-0.05	-0.08	0.00	0.01	Contr #9
Contr #10	disease control	SCD								-						0.05	-0.03	-0.09	-0.05	Contr #10
Contr #11	disease control	MSA		-				-	-	-						0.27	0.13	0.22	0.06	Contr #11
Contr #12	disease control	MSA		-				+		-						0.09	0.15	0.34	0.05	Contr #12
Contr #13	disease control	SCD		-				-		-				-	-	-0.13	-0.15	0.06	-0.03	Contr #13
Contr #14	disease control	SCD		+-	n.d.			+		-						0.07	0.03	0.12†	-0.02	Contr #14
Contr #15	disease control	FTLD		-				-		-						0.07	0.19	0.04	0.08	Contr #15
Contr #16	disease control	MSA		-				-		-						0.24	0.15	0.08	0.15	Contr #16
Contr #17	disease control	MSA		-				-		-						0.09	-0.14	-0.04	0.06	Contr #17
Contr #18	disease control	SCD		-				-		-						-0.01	0.09	-0.01	-0.07	Contr #18
Contr #19	disease control	ALS		-				-		-						-0.08	-0.08	0.04	-0.01	Contr #19
Contr #20	disease control	MSA		-				-		-						-0.18	-0.11	-0.06	0.00	Contr #20
Contr #21	disease control	ALS		+-	n.d.			+		-						0.04	0.08	0.39	-0.01	Contr #21
Contr #22	disease control	PD		-				-		-						0.12	-0.03	0.09	-0.02	Contr #22
HC #1	healthy control															0.01	0.03	0.00	0.08	HC #1
HC #2	healthy control															0.08	−0.09	0.11	0.12	HC #2
HC #3	healthy control															0.20	0.10	0.08	0.04	HC #3
HC #4	healthy control															0.07	0.00	0.04	−0.05	HC #4
HC #5	healthy control															0.14	−0.04	−0.02	0.13	HC #5
HC #6	healthy control															0.01	−0.08	−0.18	−0.07	HC #6
HC #7	healthy control															0.09	0.07	0.06	0.01	HC #7
HC #8	healthy control															−0.11	−0.03	−0.01	0.02	HC #8
HC# 9	healthy control															0.02	−0.05	−0.04	−0.06	HC# 9
HC #10	healthy control															−0.12	−0.08	0.18	0.04	HC #10
HC #11	healthy control															0.21	−0.20	0.04	−0.02	HC #11
HC #12	healthy control															0.05	0.08	0.09	0.19	HC #12
HC #13	healthy control															−0.04	−0.01	0.12	−0.07	HC #13
HC #14	healthy control															−0.04	0.07	0.09	0.08	HC #14
HC #15	healthy control															−0.07	0.05	−0.01	−0.06	HC #15
HC #16	healthy control															−0.10	0.17	0.20	0.11	HC #16
HC #17	healthy control															−0.19	−0.10	0.12	0.11	HC #17
HC #18	healthy control															0.03	0.07	0.18	0.09	HC #18
HC #19	healthy control															−0.17	−0.05	0.05	−0.01	HC #19
HC #20	healthy control															−0.03	−0.10	0.02	0.01	HC #20
HC #21	healthy control															−0.20	0.00	0.06	0.00	HC #21
HC #22	healthy control															0.12	−0.03	0.16	−0.06	HC #22
HC #23	healthy control															0.01	0.14	0.14	0.10	HC #23

HC, healthy control; VGKC-Ab, VGKC-complex antibodies; HP, hippocampal neurons; ++, strongly positive; +, positive; +-, slightly positive; -, negative; n.d., bands were analyzed but specific proteins were not determined; LE, limbic encephalitis; NMT, neuromyotonia; MoS, Morvan syndrome; ALS, amyotrophic lateral sclerosis; MSA, multiple system atrophy; SCD, spinocerebellar degeneration; CBD, corticobasal degeneration; PD, Parkinson's disease; FTLD, frontotemporal lobar degeneration. (LGI1)*, P60 gel band was not subjected to LC-MS/MS analysis, but LGI1 was detected by Western blotting; **, GABAAR subunits, a1b3g2; †, false negative results in ELISA (3, 2 and 6 patients in LGI1, CASPR2 and DCC, respectively, and 1 disease control patient in DCC), which were regarded as positive through duplicated cell-based binding assays; ‡, false positive results in ELISA (3 patients in LGI1), which were regarded as negative through duplicated cell-based binding assays.

Table 3. Results of mass spectrometry

Serum #	Rank[a]	MW (kDa) in the gel	Protein[b]	LC-MS / MS		
				Probability[c]	Score[d]	Hits[e]
#1	1	170	CASPR2	4.22 E-09	206	24
#2	1	60	LGI1	5.85 E-07	242	28
	2	70	ADAM11	1.19 E-07	30	3
	3	80	ADAM23	1.94 E-04	30	3
	4	90	PSD-95	1.62 E-06	20	2
#4	1	60	LGI1	3.37 E-06	90	9
#5	1	60	LGI1	7.93 E-07	30	3
#6	1	180	DCC	1.54 E-07	266	32
	2	170	CASPR2	1.36 E-08	88	10
	3	60	LGI1	4.94 E-04	40	4
#7	1	60	LGI1	1.48 E-05	60	7
#9	1	170	CASPR2	2.60 E-08	104	12
	2	>300	ODZ4	5.86 E-09	78	8
	3	>300	ODZ1	1.18 E-05	70	7
	4	>300	CSMD1	3.63 E-05	40	4
	5	60	LGI1	1.99 E-05	26	3
	6	80	ADAM23	4.98 E-06	20	2
#12	1	60	LGI1	4.47 E-06	170	21
	2	70	ADAM11	1.89 E-04	20	2
#15	1	70	ADAM11	3.64 E-06	40	4
	2	90	PSD-95[f]	9.40 E-06	40	4
		60	n.t.[g]			
#17	1	170	CASPR2	6.89 E-12	122	18
	2	180	DCC	5.28 E-10	128	13
#21	1	170	CASPR2	1.42 E-08	66	8
	2	180	DCC	5.74 E-10	46	5
		60	n.t.[g]			
#24	1	180	DCC	6.99 E-08	186	21
	2	90	DPP10	2.13 E-05	154	16
	3	110	DPP6	1.49 E-06	136	14
		60	n.t.[g]			
#27	1	170	CASPR2	7.47 E-09	172	22
	2	90	DPP10	5.35 E-06	198	21
	3	110	DPP6	2.49 E-09	146	15
		60	n.t.[g]			
#32	1	48	$GABA_AR$ $\alpha 1$	6.12 E-09	80	10

		60	n.t.[g]			
#35	1	60	LGI1	5.87 E-05	30	3
#40	1	100	GluA1	1.65 E-07	182	22
	2	100	GluA2	1.48 E-07	200	21
#53	1	100	GluA1	1.77 E-06	220	24
	2	100	GluA2	1.44 E-07	192	20
	3	100	GluA4	5.86 E-06	44	5
#56	1	100	GluA2	5.29 E-08	106	11
	2	100	GluA1	4.96 E-06	100	10
	3	100	GluA3	4.97 E-04	30	3
	4	100	GluA4	5.15 E-04	30	3
#63	1	180	DCC	2.01 E-10	60	6
		60	n.t.[g]			
#64	1	160	TMEM132A	9.86 E-06	78	9
	2	60	LGI1	3.71 E-04	40	4
#65	1	60	LGI1	2.36 E-04	40	4
#72	1	90	DPP10	4.42 E-05	60	7
	2	110	DPP6	1.98 E-04	10	2
		60	n.t.[g]			
#78	1	100	GluA1	1.06 E-07	122	13
	2	100	GluA2	1.00 E-05	108	12
	3	90	DPP10	8.88 E-05	106	12
	4	110	DPP6	1.07 E-04	60	6
	5	100	GluA3	1.65 E-05	20	2
#133	1	100	GluA1	5.00 E-09	140	14
	2	100	GluA2	2.92 E-08	120	12
	3	100	GluA4	5.87 E-06	48	6
#136	1	60	LGI1	1.26 E-05	40	4
#144	1	180	DCC	8.78 E-08	154	18
#148	1	60	LGI1	3.33 E-05	70	7
	2	35	$K_V\beta2$[f]	5.19 E-05	20	2
#149	1	60	LGI1	3.93 E-07	68	7
#154	1	170	CASPR2	3.16 E-06	114	14
	2	65	GAD65[f]	2.78 E-08	92	11
#160	1	160	GluN3B	1.50 E-04	18	2
#161	1	60	LGI1	9.01 E-05	50	5

[a]Proteins are ranked by peptide hits. [b]Cell-surface proteins identified with probability value (<1.0 E-04) and score (>20) are listed. [c]Probability of finding a match as good as or better than the observed match by chance. [d]SEQUEST scores. [e]Number of unique parent peptides found. [f]GAD65, $K_V\beta2$ and PSD-95 are

intracellular proteins, but have been related to immune-mediated neurological disorders or to the cell-surface antigens. [g]n.t., p60 band was not tested by mass spectrometry, but LGI1 was detected by Western blotting. LC-MS/MS, liquid chromatography-coupled tandem mass spectrometry.

Table 4. List of autoantigens identified in this study

Autoantigens	Associated disease in this study[a]	Method	MW (kDa)	Known function and associated disease	Remarks
LGI1	LE (32); NMT (11); MoS (1)	IP/IF	64	Regulation of AMPAR Epilepsy (ADLTE)	
CASPR2	NMT (9); LE (4); MoS (1)	IP/IF	148	Axon-glial interaction K^+channel clustering Autism	
GluAs	LE (2); Others (encephalitis 3)	IP/IF	102/ 99	Excitatory synaptic transmission Synaptic plasticity	
DCC	LE (8); NMT (7); MoS (1); Others (MG 1, encephalitis 1); MSA (1); SCD (1); ALS (1)	IP/IF	158	Axon guidance Receptor for Netrin-1	
DPP10	LE (1); NMT (2); MoS (1); Others (encephalitis 1)	IP/IF	91	Regulation of Kv4.2 Asthma	DPP6 was always co-immunoprecipitated
$GABA_AR$ subunits	LE (2)	IP/IF	54/61	Inhibitory synaptic transmission Epilepsy	
ADAM23	LE (1)	IF	92	Receptor for LGI1 Epilepsy	
CSMD1	LE (1)	IP/IF	388	Schizophrenia	
ODZ1	LE (1)	IP/IF	305	Bipolar disorder	Also known as Teneurin-1 ODZ4 was co-immuno-precipitated, but the direct serum binding was not tested
TMEM132A	LE (1)	IP/IF	110		

IP, immunoprecipitation; IF, immunofluorescence assay; LE, limbic encephalitis; NMT, neuromyotonia; MoS, Morvan syndrome; MG, myasthenia gravis; MSA, multiple system atrophy; SCD, spinocerebellar degeneration; ALS, amyotrophic lateral sclerosis.

[a] Numbers indicate frequency based on the cell-based IF assay.

Table 5. Relationship between clinical features and autoantibodies to LGI1, CASPR2, DCC and DPP10

	Total	LGI1 (>0.8)		LGI1 alone (>0.8)		CASPR2 (>0.3)		DCC (>0.3)		DPP10 (>0.4)	
	n=145	n=34	*P**	n=28	*P**	n=12	*P**	n=12	*P**	n=5	*P**
Clinical features											
Memory loss	77	27	0.0004	23	0.0006	4	NS	5	NS	3	NS
Confusion	82	26	0.0106	22	0.0187	4	NS	5	NS	3	NS
Seizures†	62	22	0.0052	21	0.0002	2	NS	1	NS	1	NS
Neuromyotonia†	42	6	NS	2	NS	11	<0.0001	7	0.0404	4	0.0255
Thymoma†	18	8	0.0372	3	NS	10	<0.0001	10	<0.0001	4	0.0008
Myasthenia gravis	5	1	NS	0	NS	3	0.004	5	<0.0001	2	0.0092
Any dysautonomia‡	27	6	NS	4	NS	6	0.0178	5	NS	3	NS
VGKC-Ab (≥400 pM)	69	32	<0.0001	26	<0.0001	11	0.0016	11	0.0016	4	NS
Diagnosis											
LE	59	29	<0.0001	26	<0.0001	3	NS	4	NS	1	NS
NMT/MoS	35	5	NS	2	NS	9	<0.0001	7	0.0086	3	NS
Others	51	0	NS	0	NS	0	NS	1 (MG)	NS	1 (E)	NS

Numbers indicate frequency based on the ELISA assay. *The association between individual autoantibodies and particular clinical features or diagnoses of patients was analyzed with Fisher's exact test. NS=not significant. †Data available for 144 patients. ‡Data available for 130 patients. VGKC-Ab, VGKC-complex antibodies; MG, myasthenia gravis; E, Encephalitis.

Table 6. Cut-off values of anti-LGI1-ELISA for the diagnosis of LE

LGI1 cut-off value	Sensitivity[a] (%)	Specificity[b] (%)	False positive rate[c] (%)	PPV[d] (%)	*P* value[e]
1.2	33.9	100	0	100	6.69 E-08
1.0	44.1	100	0	100	7.45 E-10
0.8	**49.2**	**94.2**	**5.8**	**85.3**	**1.19 E-07**
0.6	49.2	90.7	9.3	78.4	3.06 E-06
0.4	52.5	79.1	20.9	63.3	0.0013
0.2	64.4	54.7	45.3	49.4	0.12

[a]Sensitivity, the percentage of patients positive for LGI1 antibodies among patients diagnosed with LE; [b]Specificity, the percentage of patients negative for LGI1 antibodies among non-LE patients; [c]False positive rate, the percentage of non-LE patients who test positive for LGI1 antibodies, equal to (100-specificity); [d]Positive predictive value (PPV), the percentage of the patients diagnosed with LE among the patients positive for LGI1. [e]*P* value = Chi-square test. The frequencies of LE patients were compared between patients positive for LGI1 and all 145 patients. To predict LE patients from LGI1-ELISA data, the best cut-off point was sought, using the receiver operating characteristic (ROC) curve composed of sensitivity and false positive rate. Cut-off value of 0.8 determined by the highest sensitivity and the lowest false positive rate provided the high PPV, indicating the good predictor of LE.

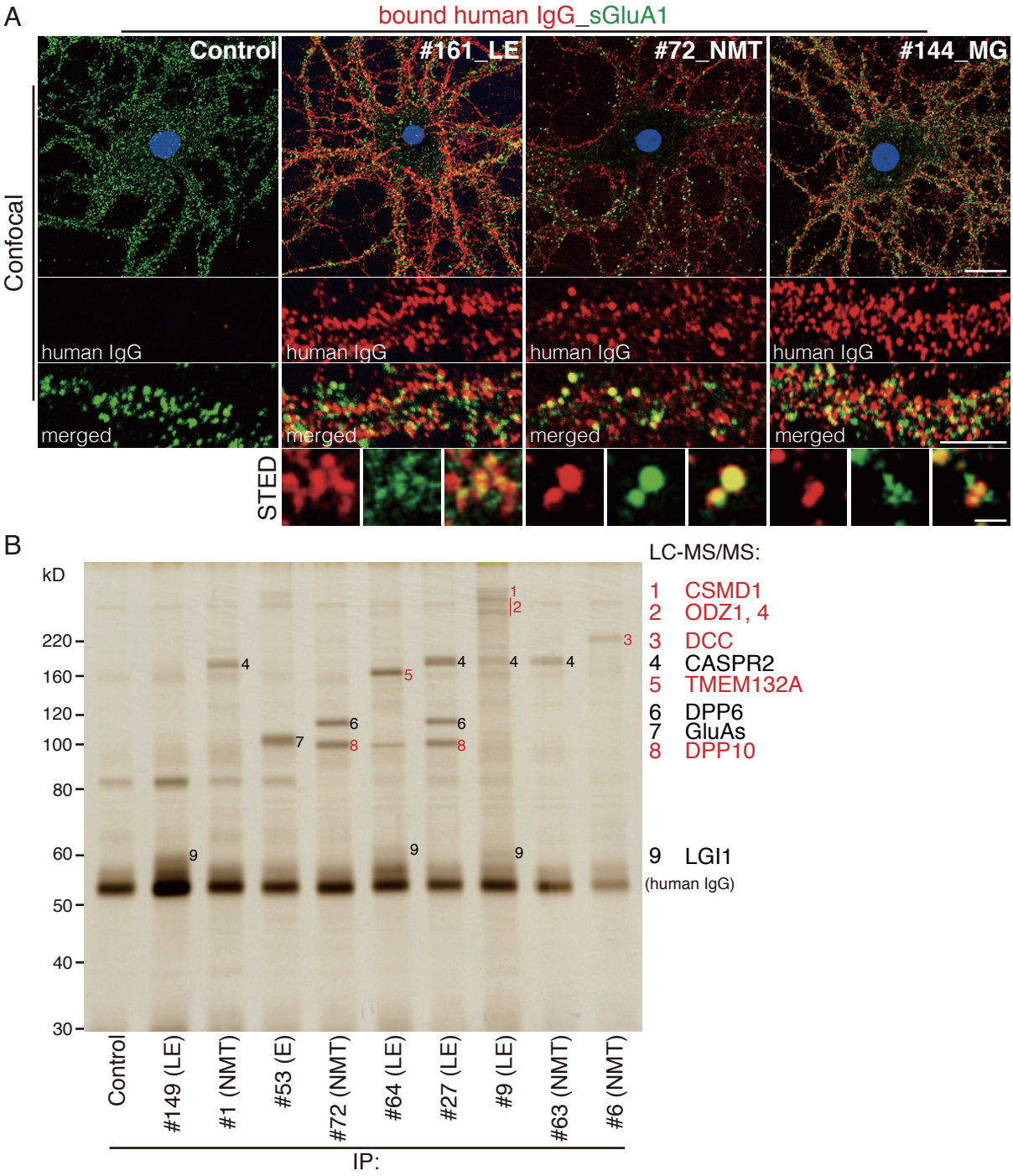

Figure 1. Systematic identification of cell-surface autoantigens targeted in neuroimmunological disorders.

A, The differential reactivity of serum antibodies to hippocampal neurons. I screened the sera from patients that strongly bind to the neuronal cell surface. Live rat hippocampal neurons were incubated with the individual sera (1:100 dilution) and an antibody to the extracellular epitope of GluA1. Surface GluA1 (sGluA1, green) and bound human IgG (red) were visualized by confocal or STED microscopy. Representative serum results are shown. Subsequent experiments revealed that sera #161, #72, and #144 included LGI1, DPP10, and DCC antibodies, respectively. Scale bars, 20 µm (upper); 5 µm (middle); 0.5 µm (lower).

B, The isolation of autoantibody-mediated immunecomplexes from cultured hippocampal neurons. Live rat hippocampal neurons were incubated with the indicated sera (1:50 dilution). Isolated immunecomplexes were separated by SDS-PAGE, followed by silver staining. Specific protein bands were analyzed by the LC-MS/MS for protein identification (protein name: black, known antigens; red, novel antigen candidates). Representative serum results are shown.

LE, limbic encephalitis; NMT, neuromyotonia; E, encephalitis; IP, immunoprecipitation.

Figure 1 Ohkawa

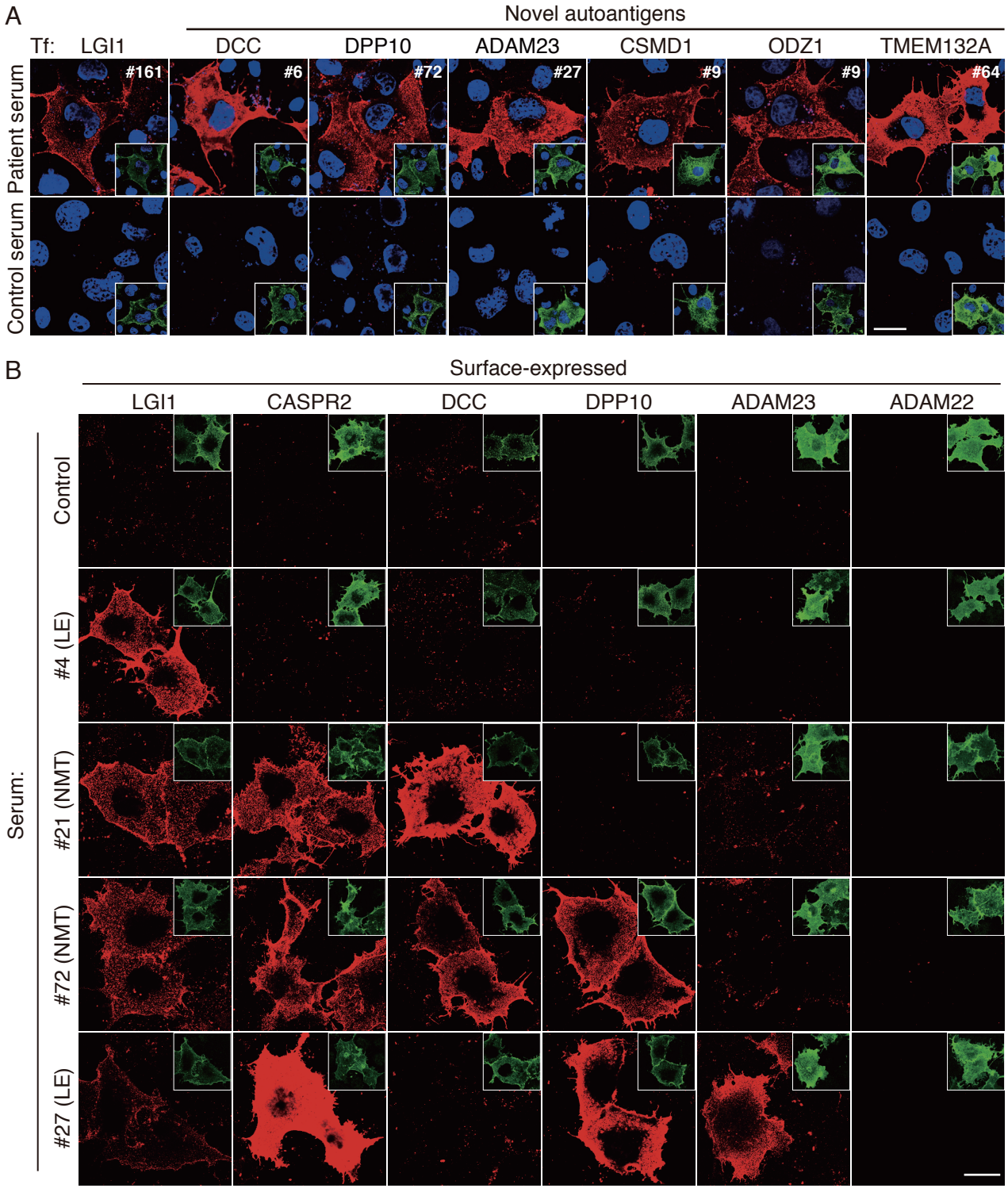

Figure 2-1 Ohkawa

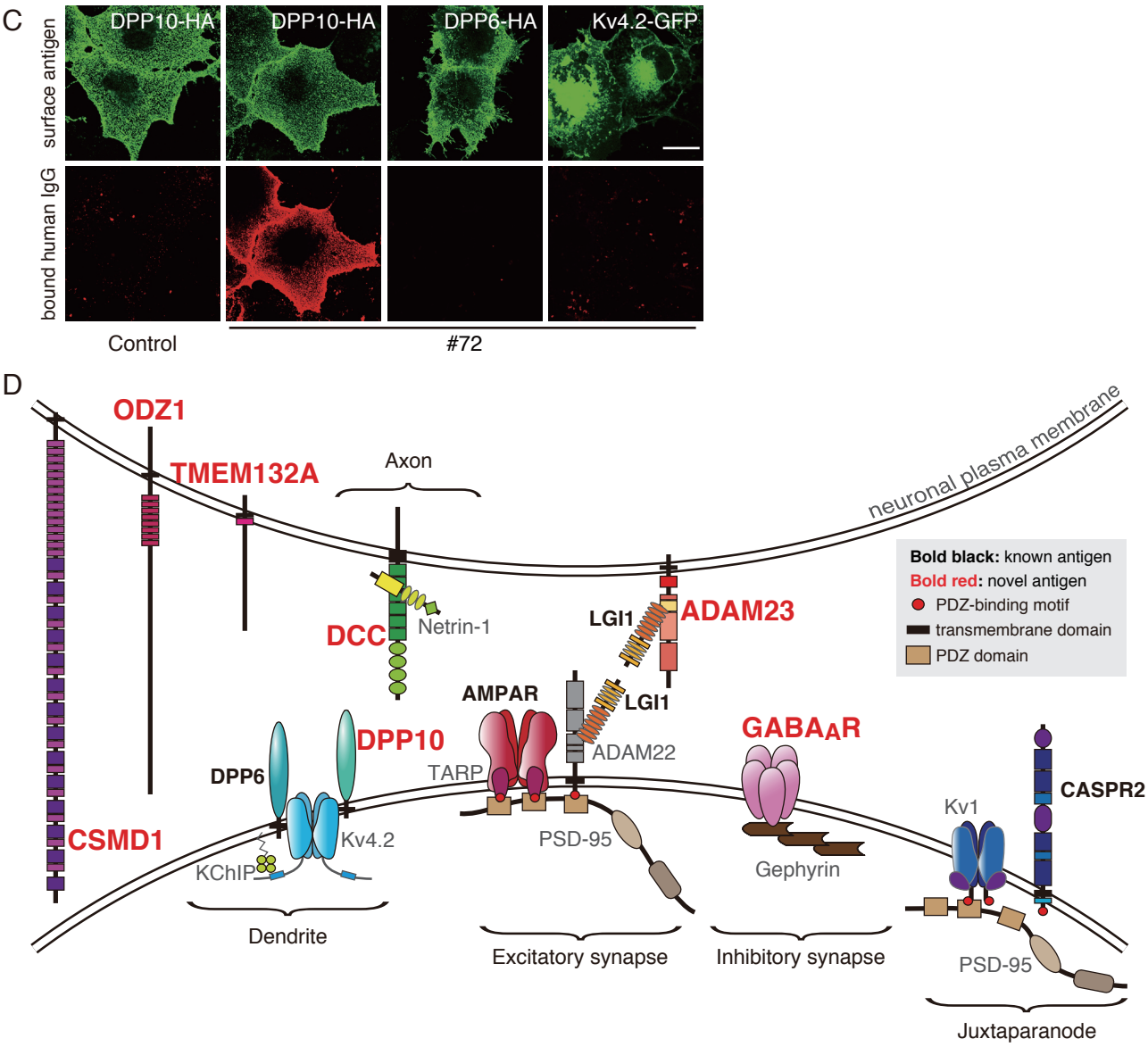

Figure 2. Determination of novel autoantigens by the cell-based binding assay.

A, COS7 cells were transfected (Tf) to surface-express the indicated antigens. Transfected cells were fixed and doubly stained with the patient serum (1:10 dilution) (bound human IgG, red) together with the antibody to surface-expressed antigen (green in insets). Nuclear DNA was stained by Hoechst 33342 (blue) to distinguish untransfected cells. Representative serum results are shown.

B, Multiple cell-surface proteins are targeted in some patients. The indicated sera from patients were examined for binding to surface-expressed antigen panels of LGI1, CASPR2, DCC, DPP10, ADAM23 and ADAM22-expressing COS7 cells (bound human IgG, red; surface-expressed antigens, green in insets). None of the sera showed binding to ADAM22.

C, DPP10, but neither DPP6 nor Kv4.2, is a direct target antigen. All five sera positive to DPP10 (#18, #24, #27, #72, and #78) showed no reactivity to DPP6 or Kv4.2. Representative serum results are shown (#72, NMT). Scale bars, 20 μm (**A**–**C**).

D, The cell-surface and synaptic autoantigens identified in this study are illustrated. These proteins are located at specific membrane domains of neurons: pre- and postsynaptic membranes for AMPAR, LGI1, ADAM23 and $GABA_AR$; juxtaparanodes for CASPR2; and axon terminals for DCC. Bold text, targeted antigens (black, known and red, novel); narrow text, interacting or related proteins with antigens.

Figure 2-2 Ohkawa

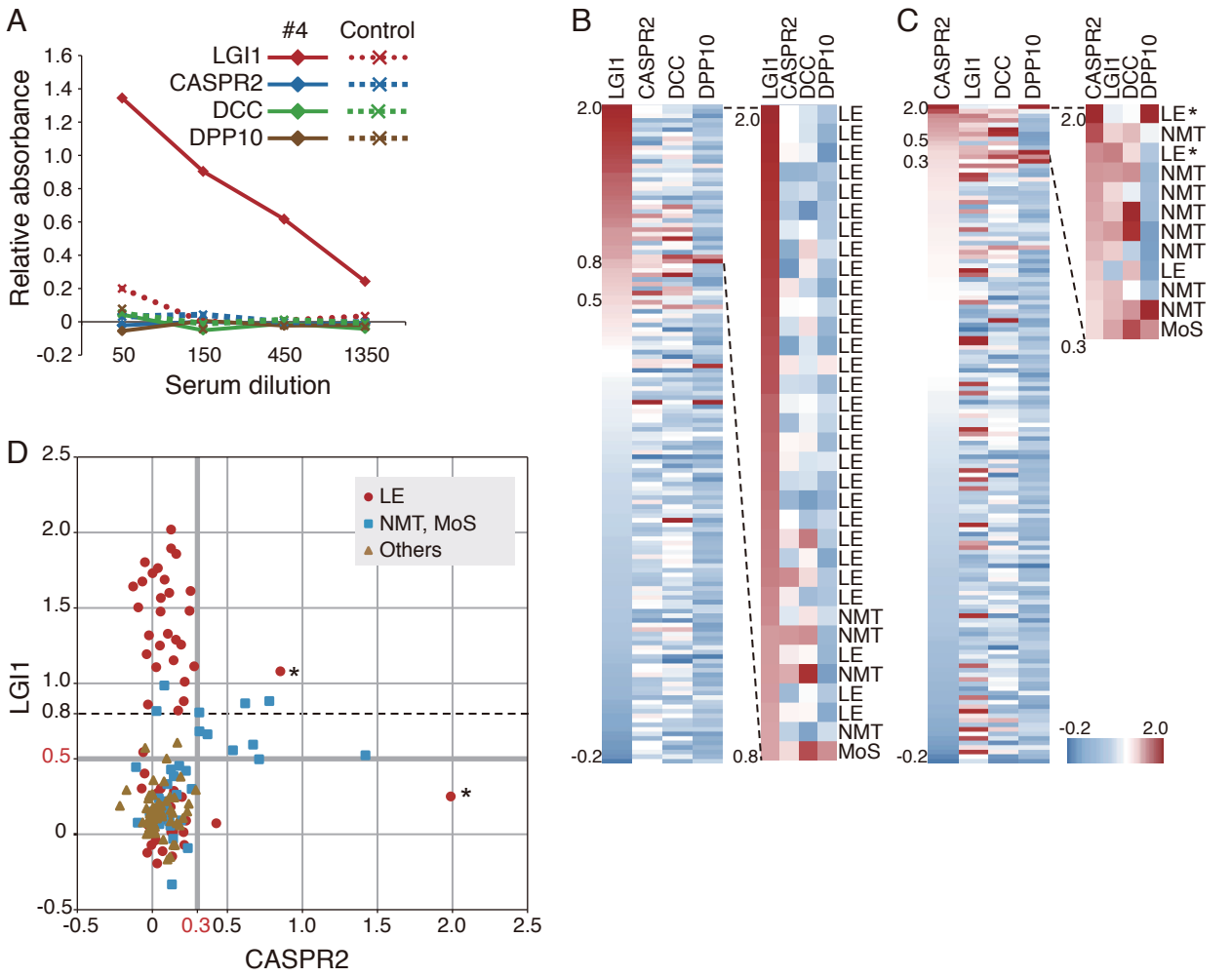

Figure 3. Multiple cell-based ELISA testing reveals an exclusive role for LGI1 antibodies in LE.

A, Cell-based ELISA tests against LGI1, CASPR2, DCC and DPP10 show the adequate signal-to-noise ratio. A representative serum #4 (patient with LE) showed positive reactivity only to LGI1 but not to CASPR2, DCC or DPP10. I confirmed a linear relationship between the relative absorbance and the serum dilution factor (1:50 to 1:1350 dilution) in all sera tested. The control serum tested showed no significant binding to any antigens (dashed lines). The relative absorbance at a dilution of 1:50 was used as the antibody value for an individual patient.

B, **C**, LGI1 antibodies occur in LE independently from other antibodies. Heat maps were generated from datasets of all the patients (145 patients). The individual data of the patient serum for LGI1-CASPR2-DCC-DPP10 ELISA (**B**) or CASPR2-LGI1-DCC-DPP10 ELISA (**C**) are shown in the horizontal columns, and sorted in descending order of the anti-LGI1 (**B**) or anti-CASPR2 (**C**) values (-0.2 to 2.0). The top groups with high LGI1-ELISA (> 0.8) (**B**) and with high CASPR2-ELISA (> 0.3) (**C**) values are shown in magnified views with the individual diagnosis (LE, NMT or MoS).

D, Scatterplot showing the relationship between LGI1 and CASPR2 antibody values in patients with LE (red circles), NMT (blue squares) or Others (brown triangles). Asterisks indicate the cases in which the patients were originally diagnosed with LE but experienced NMT symptoms (#9 and #27, revealed by retrospective examination) (**C** and **D**).

Figure 3 Ohkawa

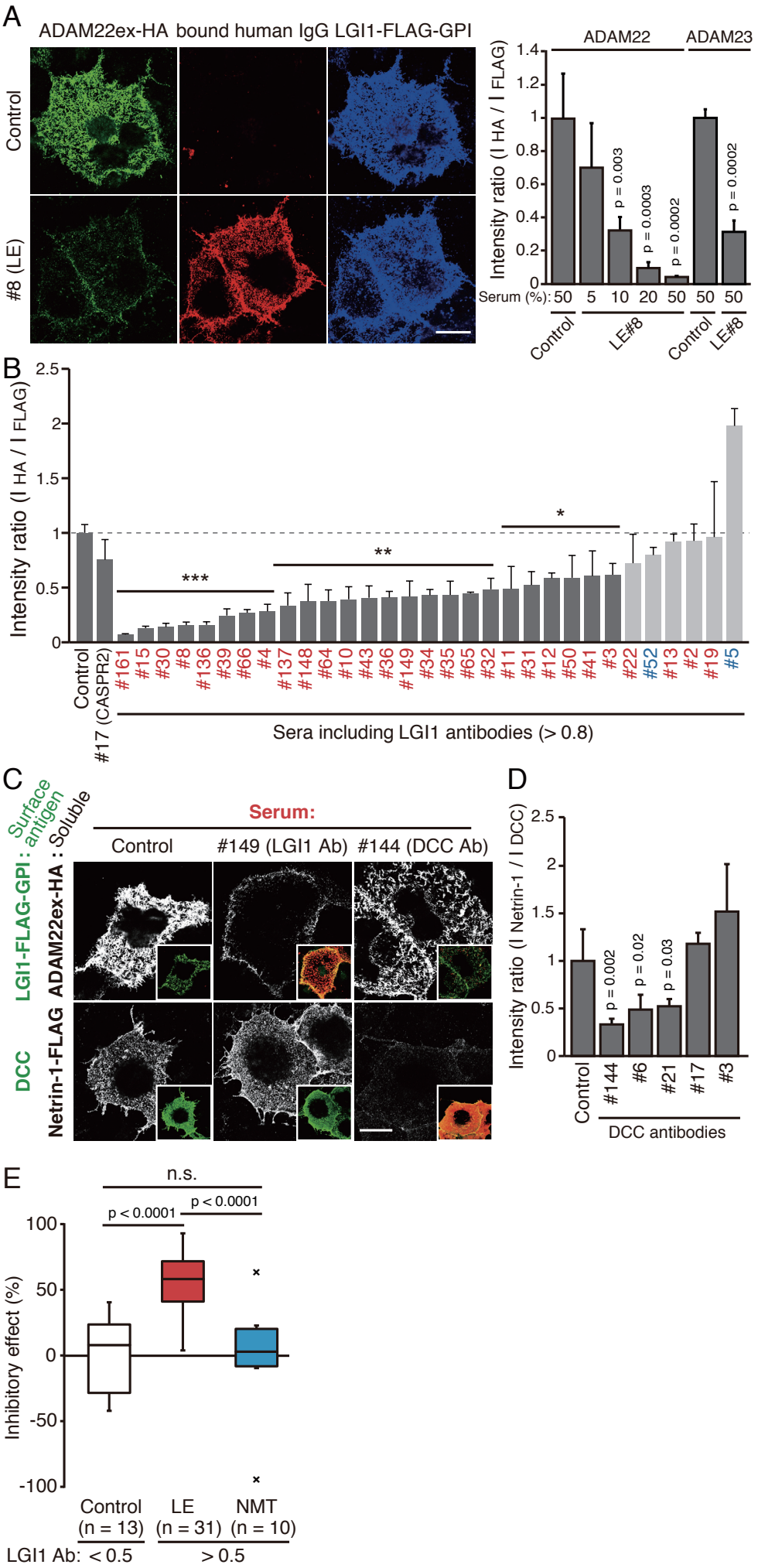

Figure 4-1 Ohkawa

Figure 4. LGI1 autoantibodies associated with LE inhibit the interaction of LGI1 with ADAM22.

A, **B**, COS7 cells transfected with LGI1-FLAG-GPI were incubated with patient or control sera. Then, the soluble form of ADAM22 or ADAM23 (ADAMex-HA) was added. Bound ADAM22ex-HA (green), surface-expressed LGI1-FLAG-GPI (blue) and bound human IgG (red) were visualized without cell permeabilization. (**A**) Serum from patient #8 with LE inhibited the interaction of LGI1 with ADAM22 in a dose-dependent manner. Scale bar, 20 μm. Error bars show ± SD. (**B**) Most of the sera from patients with monospecific LGI1 antibodies (absorbance > 0.8 in ELISA) inhibited the interaction of LGI1 with ADAM22. A limited number of serum samples with high levels of LGI1 antibodies did not show the inhibition under the condition (light gray). Red text, patients with LE; blue text, patients with NMT. Error bars show ± SEM (n = 3). *P < 0.05; **P < 0.01; ***P < 0.001.

C, Serum from an MG patient with monospecific antibodies to DCC (#144) specifically inhibited the interaction between DCC and its ligand Netrin-1. Bound ADAM22ex-HA or Netrin-1-FLAG is shown (gray scale), and the merged images of surface-expressed LGI1-FLAG-GPI or DCC (green) and bound human IgG (red) are shown in insets. Scale bar, 20 μm.

D, The inhibitory effect on the DCC-Netrin-1 interaction was shared with DCC antibodies from NMT patients (#6 and #21). Error bars show ± SD. Statistical analyses were performed by one-way ANOVA followed by Dunnett's post hoc analysis (**A, B,** and **D**).

E, The inhibitory effect of LGI1 antibodies on the LGI1-ADAM22 interaction is specifically observed in sera from patients with LE, but not with NMT. LGI1 antibody (Ab)-positive patient sera (absorbance > 0.5 in ELISA) with LE or NMT were tested as in (**B**), and their induced reductions in the LGI1-ADAM22 interaction are shown as the inhibitory effect (%). Statistical analyses were performed by one-way ANOVA followed by Tukey's post hoc analysis. n.s., not significant.

Figure 4-2 Ohkawa

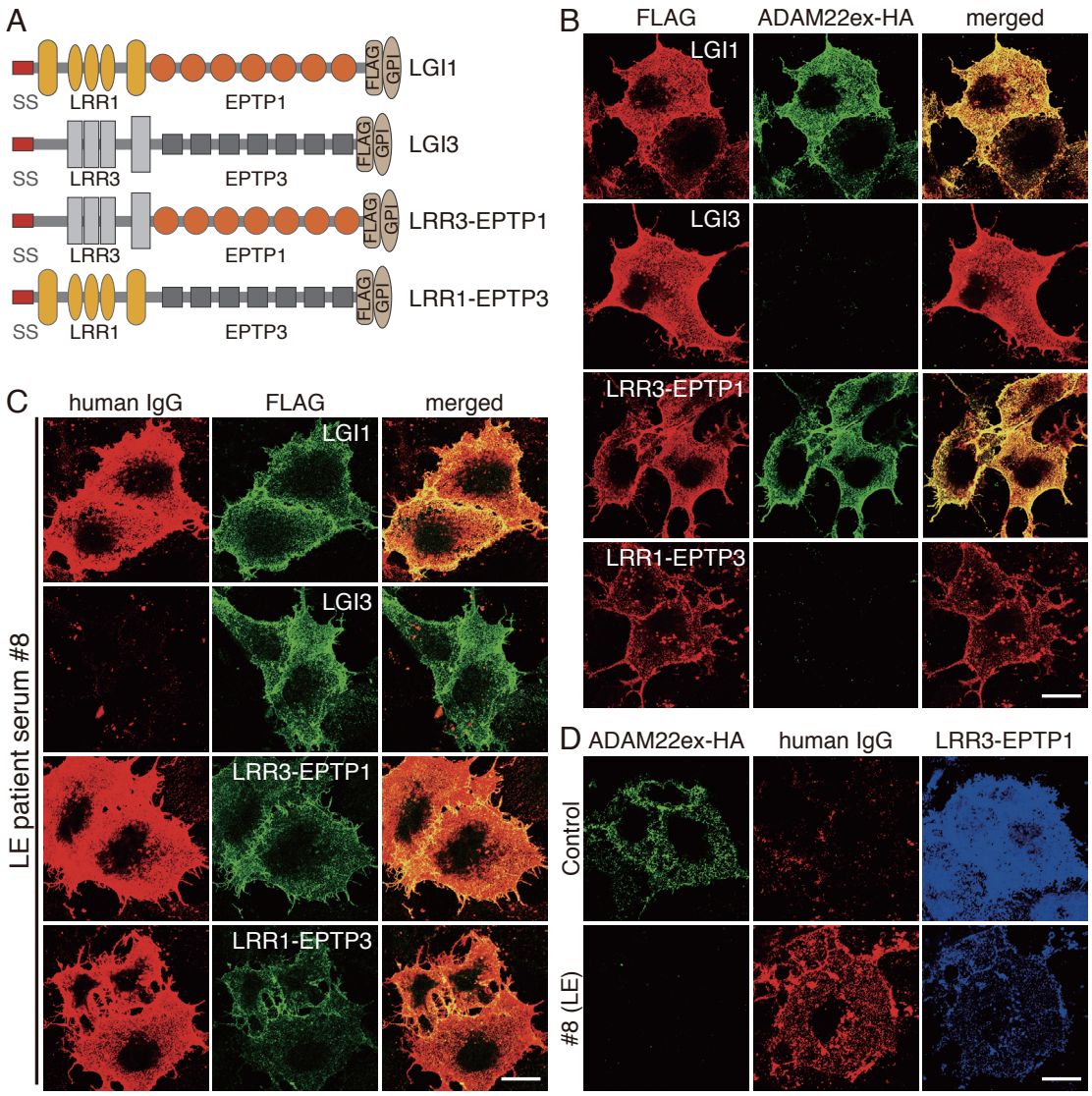

Figure 5. LGI1 antibodies inhibit the LGI1 binding to ADAM22 by neutralizing the ADAM22-binding domain of LGI1.

A, Chimeric constructs to determine the epitope in LGI1 recognized by LGI1 autoantibodies. SS, signal sequence; LRR1 or 3, LRR domain of LGI1 or LGI3; EPTP1 or 3, EPTP repeat domain of LGI1 or LGI3.

B, Binding of soluble ADAM22ex-HA (green) onto the cell-surface of COS7 cells expressing indicated chimeric LGI-FLAG-GPI constructs (red). The EPTP repeat domain of LGI1 (EPTP1) specifically mediated the ADAM22-binding.

C, All patient sera with LGI1 antibodies tested contained the polyclonal LGI1 antibodies recognizing both LRR and EPTP repeat domains of LGI1, but did not bind to any domains of LGI3. Bound human IgG and surface-expressed LGI-FLAG-GPI are shown in red and green, respectively. Representative results of serum #8 (LE) are shown.

D, COS7 cells were transfected with LRR3-EPTP1-FLAG-GPI and subjected to the assay same as Fig. 4A. Serum antibodies (#8) (red) bound to the LRR3-EPTP1 (blue) and inhibited the binding of LRR3-EPTP1 with ADAM22 (green).

Scale bars, 20 μm (**B**–**D**).

Figure 5 Ohkawa

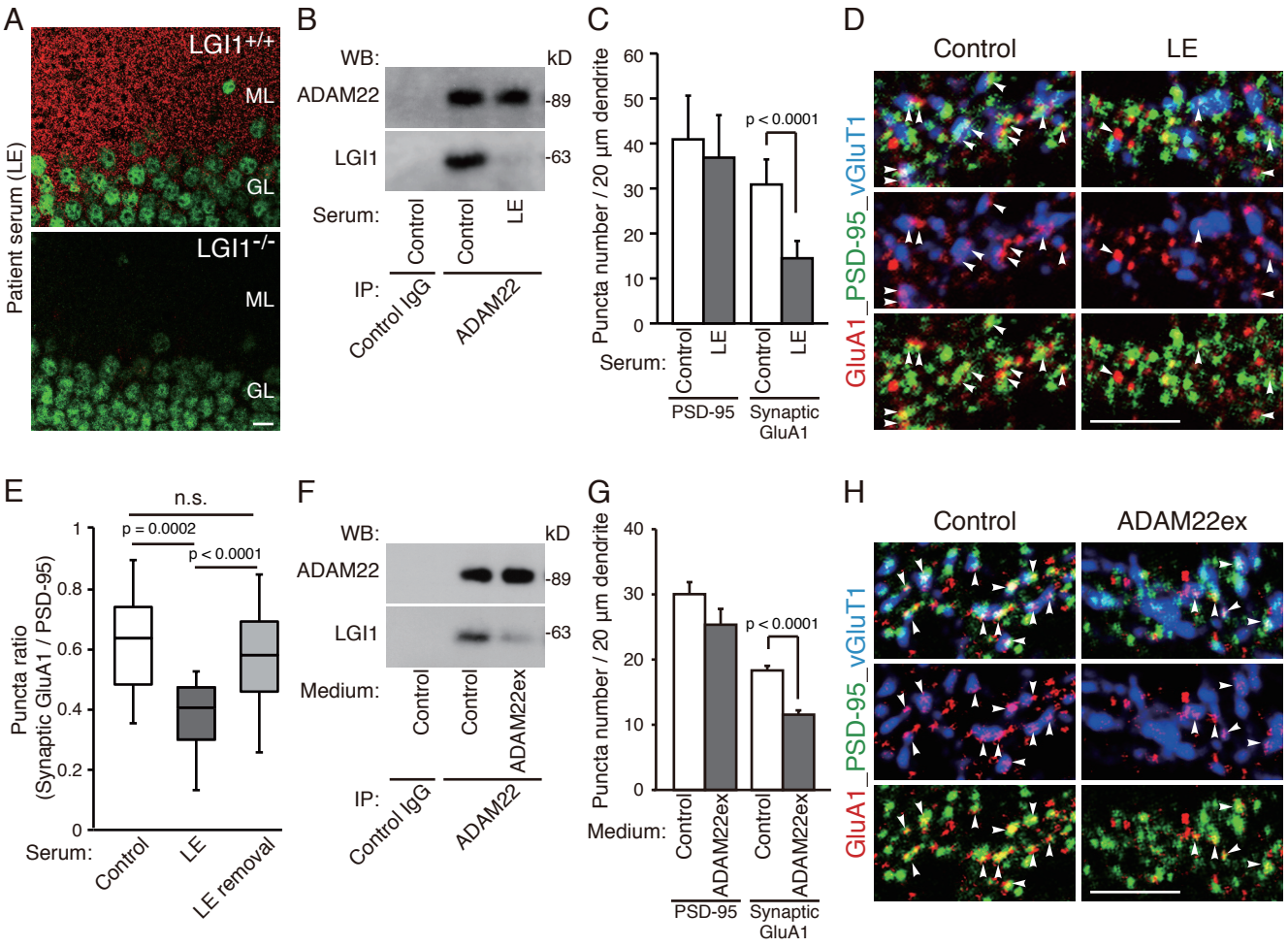

Figure 6-1 Ohkawa

Figure 6. LGI1 antibodies reduce synaptic AMPARs by blocking the LGI1-ADAM22 interaction in neurons.

A, Brain sections of the wild-type ($LGI1^{+/+}$, upper) and LGI1 KO ($LGI1^{-/-}$, lower) mice were incubated with the serum from a patient with LE (#161). The patient serum showed a strong punctate labeling (red) in neuropils of dentate gyrus in the wild-type mouse, whereas all the reactivity was abolished in the LGI1 KO mouse, indicating that the patient serum antibodies were specifically directed against LGI1. Prox1 was visualized (green) to mark granule cell nuclei. ML, molecular layer; GL, granule cell layer. Scale bar, 10 μm.

B, Cultured hippocampal neurons were incubated with the patient serum (#161, LE) or control serum (Control #19) for 3 days. ADAM22 was immunoprecipitated by ADAM22 antibody-conjugated beads. Samples of immunoprecipitates (IP) were analyzed by Western blotting (WB).

C–**E**, LGI1 autoantibodies reversibly reduce synaptic AMPARs in hippocampal neurons. Representative images of surface GluA1 clusters (red) in neurons treated with control or the patient (LE, #161) serum are shown (**D**). The number of synaptic GluA1 clusters (arrowheads), which were apposed to both vGluT1 (blue) and PSD-95 (green), was significantly reduced by the treatment with patient serum. n = 3 experiments (**C**). The reduction of synaptic GluA1 was reversed after the patient serum was removed. n = 24 dendrites from two independent experiments. Statistical analyses were performed by one-way ANOVA followed by Tukey's post hoc analysis (**E**).Error bars show ± SEM. Scale bar, 5 μm.

F, Cultured hippocampal neurons were incubated with medium containing the soluble form of ADAM22 (ADAM22ex) or control medium for 3 days. Endogenous ADAM22 was then immunoprecipitated as described in (**B**).

G, **H**, The number of synaptic GluA1 was significantly reduced by the treatment with ADAM22ex. Representative images of surface GluA1 clusters (red) in neurons treated with control medium or ADAM22ex-containing medium are shown (**H**). The number of synaptic GluA1 clusters (arrowheads), which were apposed to both vGluT1 (blue) and PSD-95 (green), was significantly reduced by the treatment with ADAM22ex. n = 3 experiments (**G**). Error bars show ± SEM. Scale bar, 5 μm.

Figure 6-2 Ohkawa

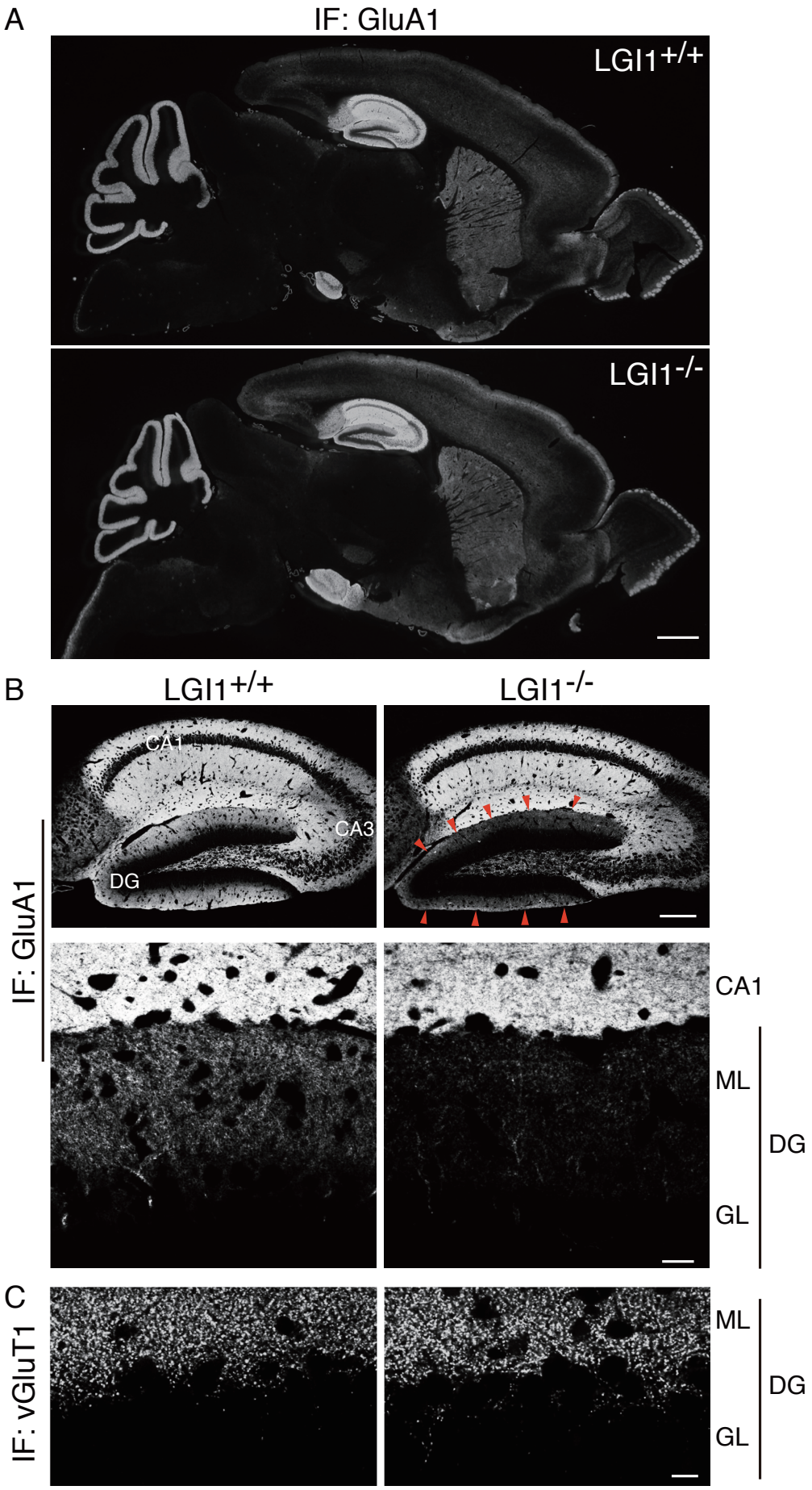

Figure 7-1 Ohkawa

Figure 7. Genetic deletion of LGI1 results in specific reduction of AMPARs in the hippocampal dentate gyrus.

A, Immunofluorescence (IF) for GluA1 subunit of AMPARs in parasagital sections of control wild-type (LGI1$^{+/+}$) and LGI1 KO (LGI1$^{-/-}$) mice.

B, Immunofluorescence for GluA1 in the hippocampus. The region including dentate gyrus (molecular and granule cell layers) and CA1 (molecular layer) was magnified (lower panels). Note a marked decrease for GluA1 in the dentate molecular layer of LGI1$^{-/-}$ mice (red arrowheads). Images from control and LGI1$^{-/-}$ mice were captured at the same gain levels. Representative data from three independent experiments are shown.

C, No changes were observed for vGluT1 immunoreactivity in the dentate molecular layer of LGI1$^{-/-}$ mice. Scale bars, 1 mm (**A**), 200 μm (**B**, upper), 20 μm (**B**, lower) and 10 μm (**C**).

DG, dentate gyrus; ML, molecular layer; GL, granule cell layer.

Figure 7-2 Ohkawa

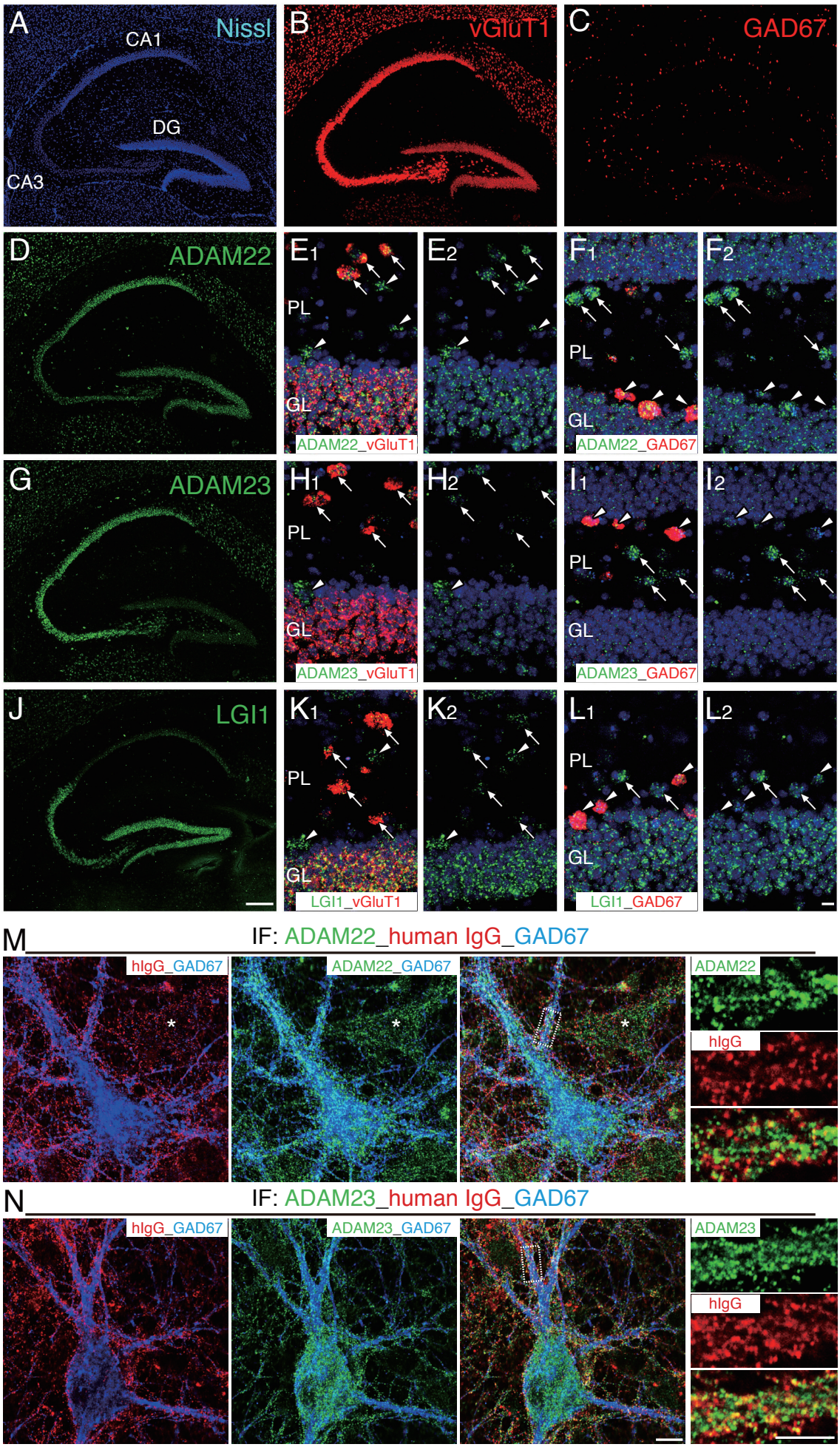

Figure 8-1 Ohkawa

Figure 8. ADAM22, ADAM23, and LGI1 are expressed in inhibitory interneurons as well as excitatory neurons in the hippocampus.

A–**L**, Double-fluorescent in situ hybridization for ADAM22, ADAM23, or LGI1 and vGluT1 or GAD67 in the mouse hippocampus. Neurons were identified with Nissl staining (**A**, **E**, **F**, **H**, **I**, **K**, and **L**; blue). vGluT1 (**B**) and GAD67 (**C)** mRNAs (red) were used as markers of glutamatergic and GABAergic neurons, respectively. ADAM22 (**D**), ADAM23 (**G**), and LGI1 (**J**) mRNAs are shown in green. The polymorphic cell layer (PL) of the dentate hilus is magnified (**E**, **F** for ADAM22; **H**, **I** for ADAM23; **K**, **L** for LGI1). Signals for ADAM22, ADAM23, and LGI1 mRNAs overlapped with those for vGluT1 (**E1**, **H1**, and **K1**; arrows) and GAD67 mRNAs (**F1**, **I1**, and **L1**; arrowheads). Arrowheads in **E**, **H**, and **K** indicate vGluT1-negative hilar neurons and arrows in **F**, **I**, and **L** indicate GAD67-negative hilar neurons. Scale bars, 200 μm (10 μm, magnified). DG, dentate gyrus; GL, granule cell layer.

M, **N**, LGI1 associates with ADAM22 and ADAM23 on hippocampal inhibitory interneurons. Rat cultured hippocampal neurons (19 DIV) were triply stained by anti-GAD67 (blue, pseudocolor), anti-ADAM22 (**M**) or ADAM23 (**N**) (green), and the patient serum [#161, human IgG (hIgG)] that was monospecific to LGI1 (red, pseudocolor). Cell-surface LGI1 signals were colocalized with ADAM22 and ADAM23 signals on GAD67-positive inhibitory interneurons (right panels, magnified view of the region indicated by dashed square). An asterisk (**M**) indicates the GAD67-negative excitatory neuron, in which ADAM22 was expressed and to which LGI1 bound. Scale bars, 10 μm (5 μm, magnified).

Figure 8-2 Ohkawa

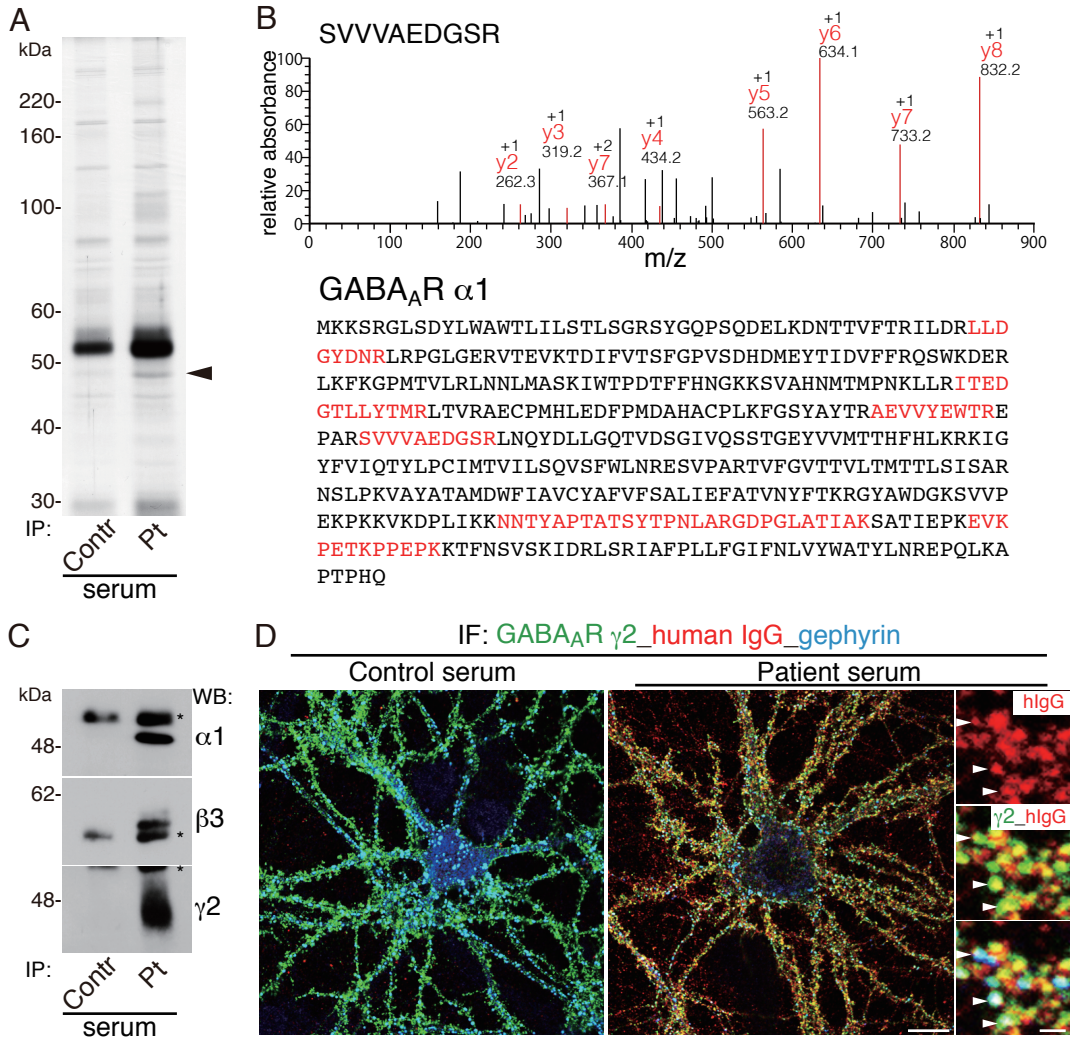

Figure 9. Identification of GABA$_A$ receptor autoantibodies in patients with limbic encephalitis.

A, Immunoprecipitation of cell-surface target proteins with patient serum antibodies (#32). The immunoprecipitates of serum antibodies bound to rat hippocampal neurons were analyzed by SDS-PAGE with silver staining. The specific band at 48 kDa (arrowhead) was analyzed by the LC-MS/MS.

B, MS/MS spectra of a peptide unique for GABA$_A$ receptor α1 subunit (m/z value of the parent ion, 509.74) obtained from the trypsinized protein band shown in A (arrowhead) (Upper panel). The matched fragment y$^+$ -ion series is indicated in red. Identified peptides in the amino acid sequence of GABA$_A$ receptor α1 are indicated in red (Lower panel). The accession number is P62813.

C, Western blotting with the subunit specific antibodies showed that α1, β3, and γ2 subunits of GABA$_A$ receptor were present in the immunoprecipitate by the patient serum antibodies. Asterisks indicate the position of the human IgG heavy chain.

D, The patient serum antibodies (#32) bind to the inhibitory GABA$_A$ receptors at the cell surface of rat hippocampal neurons. The serum reactivity (red; human IgG) was well overlapped with surface-expressed γ2 subunits of GABA$_A$ receptor (green), which were apposed to gephyrin scaffold (blue) (marked by arrowheads). Scale bars: 10 μm (1 μm, magnified).

IP, immunoprecipitation; Contr, control; Pt, patient; GABA$_A$R, GABA$_A$ receptor; WB, Western blotting; IF, immunofluorescence; hIgG, human immunoglobulin.

Figure 9 Ohkawa

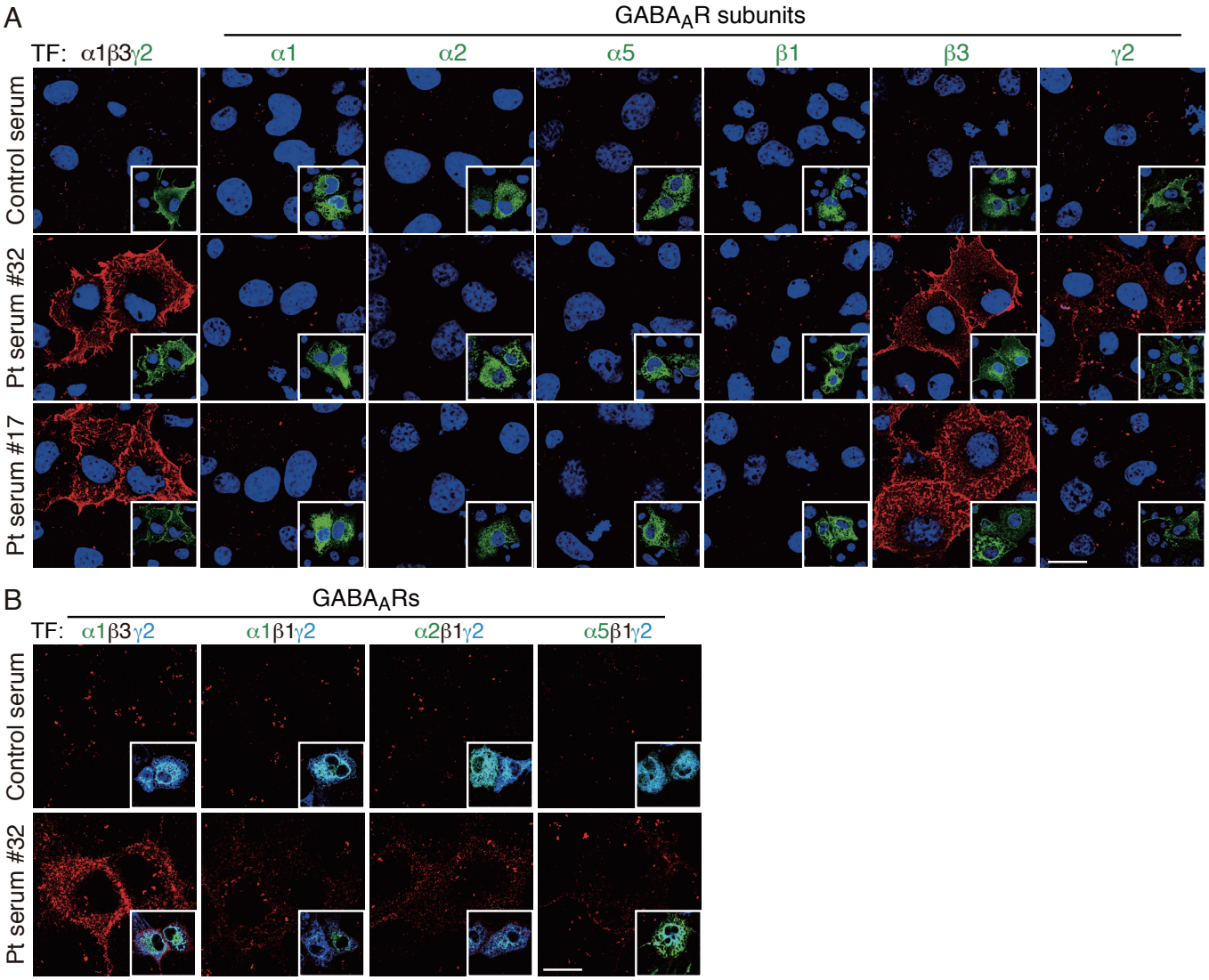

Figure 10. GABA$_A$ receptor autoantibodies are directed to extracellular epitope of β3 subunit.

A, COS7 cells were transfected (TF) to surface-express the indicated GABA$_A$ receptor subunits. Transfected cells were fixed and doubly stained with the patient sera (#32 or #17) (red) together with the antibodies specific to the individual expressed subunits (green, insets). Nuclear DNA was stained by Hoechst 33342 (blue) to distinguish untransfected cells. To clearly show the weak binding of patient serum #32 to γ2 subunit, the brightness of the red image is enhanced (the middle of the rightmost panel).

B, COS7 cells were transfected to surface-express the indicated heteromeric GABA$_A$ receptors and tested for the binding of serum antibodies (red). Transfected cells were detected by staining with the individual α subunit (green) and γ2 subunit (blue) antibodies.

Merged images are shown in insets. Scale bars: 20 μm.

Figure 10 Ohkawa

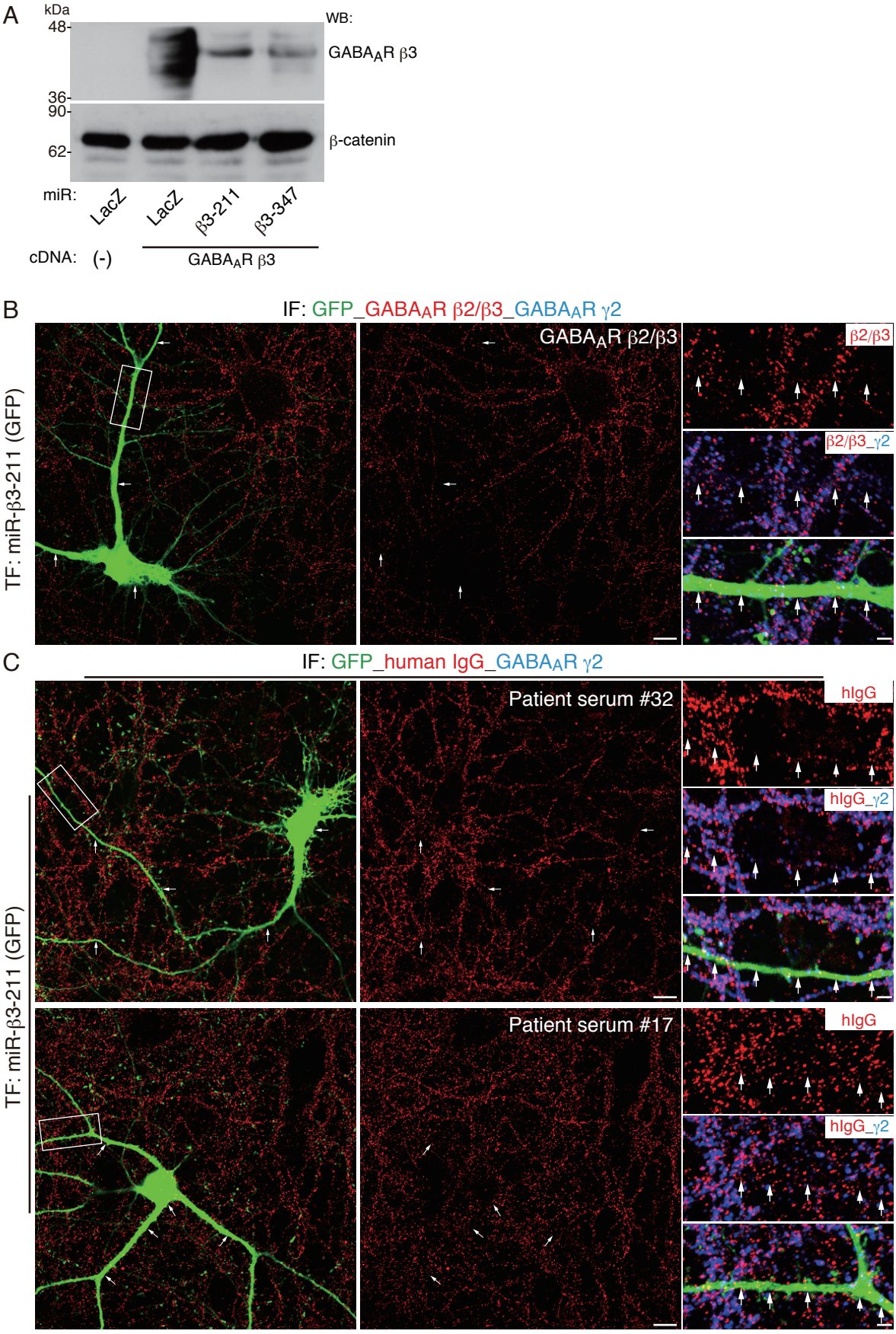

Figure 11-1 Ohkawa

Figure 11. $GABA_A$ receptor containing β3 subunit is primarily targeted in hippocampal neurons by the patients' antibodies.

A, Validation of miRNA constructs for $GABA_A$ receptor β3 subunit. HEK293T cells were co-transfected with the indicated knockdown (miR) and β3 expression vectors. Three days after the transfection, the cell lysates were analyzed by Western blotting with $GABA_A$ receptor β3 and β-catenin antibodies. miR-LacZ, control miRNA targeting to LacZ.

B, Effective knockdown of the endogenous β3 subunit. Cultured rat hippocampal neurons were transfected with the miR-β3 expression vector at 10 DIV. Cell-surface $GABA_A$ receptor β2/β3 (red) and γ2 (blue) subunits were stained at 15 DIV. MicroRNA-transfected neurons were reported by the GFP expression (green). Note that γ2 clusters were also abolished in neurons in which β3 subunit was knocked down.

C, Binding of serum antibodies (patient #32 and #17) (red) was examined in neurons in which β3 subunit was knocked down (green). Human IgG signals were mostly diminished together with γ2 subunit signals from the dendrite of the neuron with β3 subunit knocked-down.

Arrows indicate the soma and dendrites of the neuron in which β3 was knocked down (**B** and **C**). Scale bars: 10 μm (2 μm, magnified).

Figure 11-2 Ohkawa

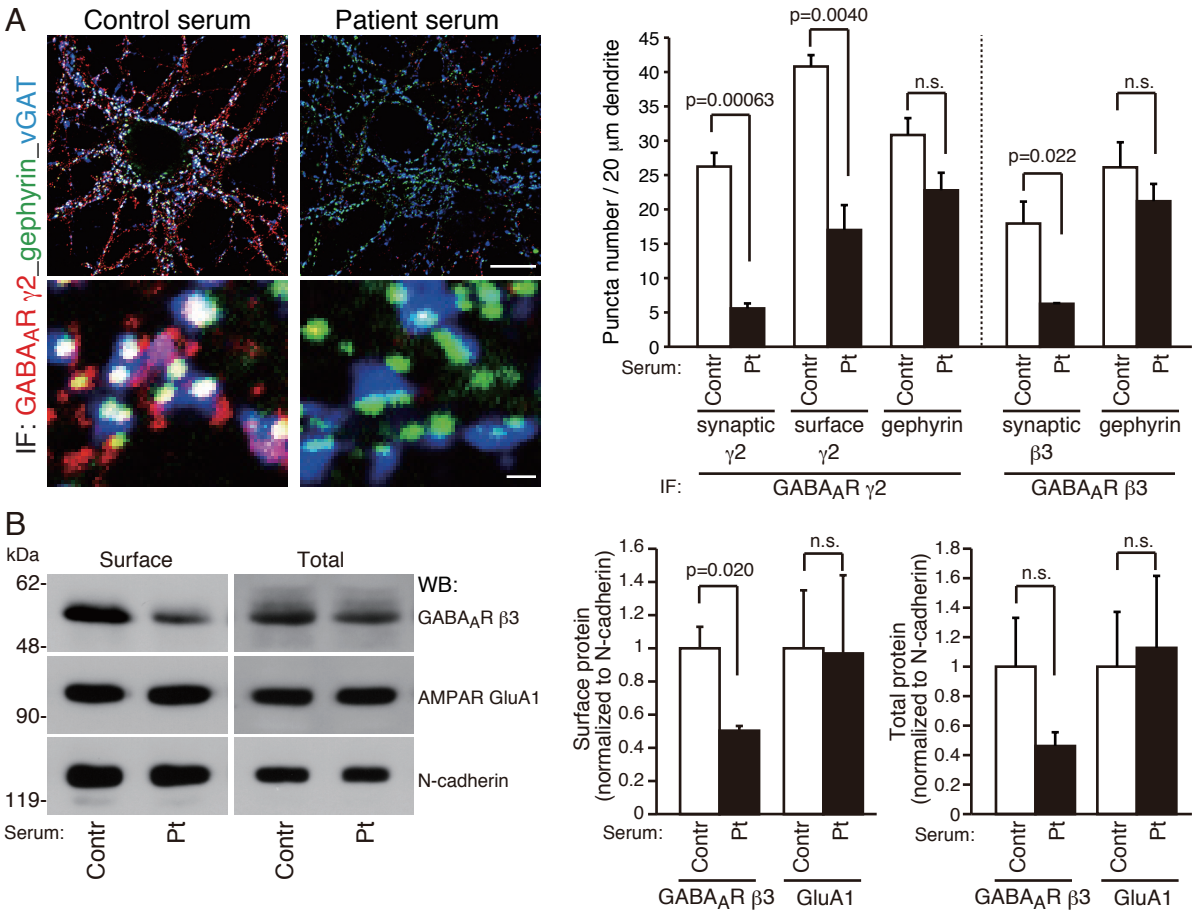

Figure 12. $GABA_A$ receptor autoantibodies reduce synaptic and cell-surface $GABA_A$ receptor density.

A, Cultured rat hippocampal neurons were incubated with the patient serum (#32) or control serum for 2 days. Synaptic $GABA_A$ receptors, which were γ2 (red) or β3 subunit-positive clusters co-localized with both gephyrin (green) and vGAT (blue), were counted. Surface-expressed $GABA_A$ receptor clusters labeled by the γ2 subunit antibody (the extracellular epitope) and gephyrin clusters were also independently counted. Scale bars: 20 μm (1 μm, magnified).

B, Surface biotinylated and total proteins of the patient serum-treated hippocampal neurons were analyzed by Western blotting with the indicated antibodies. Patient serum significantly reduced the amount of surface-expressed $GABA_A$ receptor protein; and slightly, but not significantly, that of total $GABA_A$ receptor protein.

Statistical analyses were performed by Student's t test; n.s., not significant; error bars show ± SEM; n = 3 experiments (**A** and **B**).

Figure 12 Ohkawa

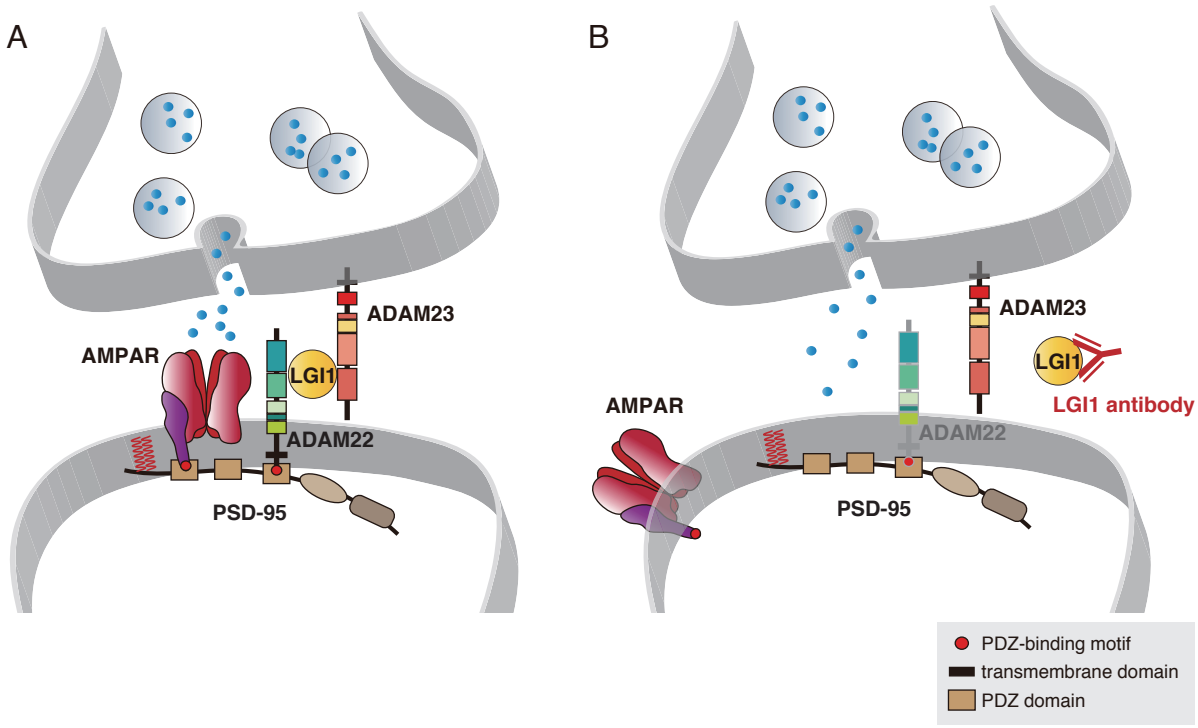

Figure 13. Schematic model of a mode of action of anti-LGI1 autoantibodies.
Effect of LGI1-ADAM22 interaction on anchoring of AMPARs at healthy (**A**) and affected (**B**) synapses is illustrated.

A, In an ordinary state, AMPARs are stably anchored at the synapse through the PDZ1 or PDZ2 domain of PSD-95, when ADAM22 binds to the PDZ3 domain of PSD-95 in the presence of LGI1.

B, In the synapses of patients with LE, LGI1-ADAM22 interaction is disrupted by anti-LGI1 autoantibodies. It can be speculated that without LGI1, ADAM22 is unstably localized at the synapse (shown in dimmed color). As a result, AMPARs are delocalized from synapses. Through such a fine regulation of synaptic AMPARs, LGI1-ADAM22 interaction maintains physiological brain excitability.

Figure 13 Ohkawa